Chapter 5

Synthesis, Characterization and Study of Novel Conjugated Molecules

Part-A: Constructing a self-assembling C_3-symmetric covalently linked (fused) donor-acceptor-type molecule containing hexaazatriphenylene core

Table of Contents

Introduction

Polycyclic aromatic hydrocarbons (PAHs) and fused polycyclic aromatic cores have captivated the researchers' interest in materials science and nanoscience owing to their tailor ability and appealing features of their electronic structures.[1] These features include extended π-conjugation, low ionization potentials, narrow band gaps and remarkable charge carrier mobilities. [2–4] It has been found that increased conjugation length improves the electronic coupling and reduces the reorganization energies in the solid state thus leading to the high charge carrier mobilities.[2,3] The *N*-substituted polycyclic aromatic analogues of PAHs have been found to be less susceptible to the degradation through oxidation of dimerization compared to the unsubstituted linear acenes (Figure 5.1).[5,6] On the other hand, large two-dimensional polycyclic aromatic compounds, that represent various fragments of graphene, have large, planar π-surfaces which can provide increased intermolecular surface overlap and effectively increase electron delocalization.[7]

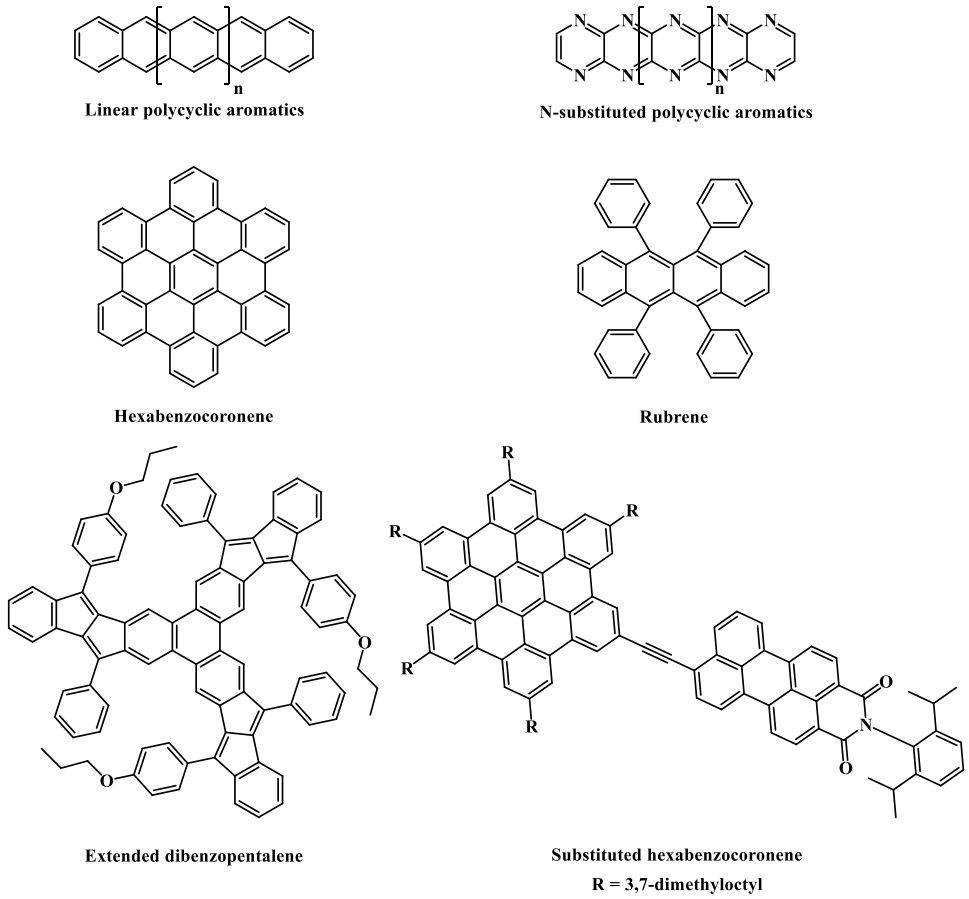

Figure 5.1 Structures of some linear PAHs[8,9] and two-dimensional PAHs like hexabenzocoronene and extended dibenzopentalene[9–11]

Many linear and star-shaped molecules comprised of the polycyclic aromatic

core and extended π-conjugation have been identified as an active component in optoelectronic devices[10,12,13] in view of their adequate HOMO and LUMO energy levels,[14,15] isotropic absorption properties and strong tendency to assemble into quasi-1D columns which in turn helps to generate a preferred charge transporting pathway.[16] The n-type and p-type semiconducting aromatic molecules having tendency to form the columnar-type π-stacked structures and self-assembled one-dimensional aggregates exhibit prominent candidature for electron and hole transporting materials[17–22] than glassy-type amorphous aromatics which show unfavourable positional and energy disorder.[23]

In the area of this research field, one of the smallest two dimensional nitrogen containing polyheterocyclic aromatic systems is the dipyrazino[2,3-*f*:2',3'-*h*]quinoxaline or 1,4,5,8,9,12-hexaazatriphenylene (**HAT**, Figure 5.2). **HAT** is an electron deficient, rigid, planar, aromatic discotic system with an excellent π-π stacking ability which has been used not only as the basic scaffold for larger two dimensional nitrogen substituted polycyclic aromatics but also as a building block of the large number of the molecular, macromolecular and supramolecular systems for a variety of applications.[9]

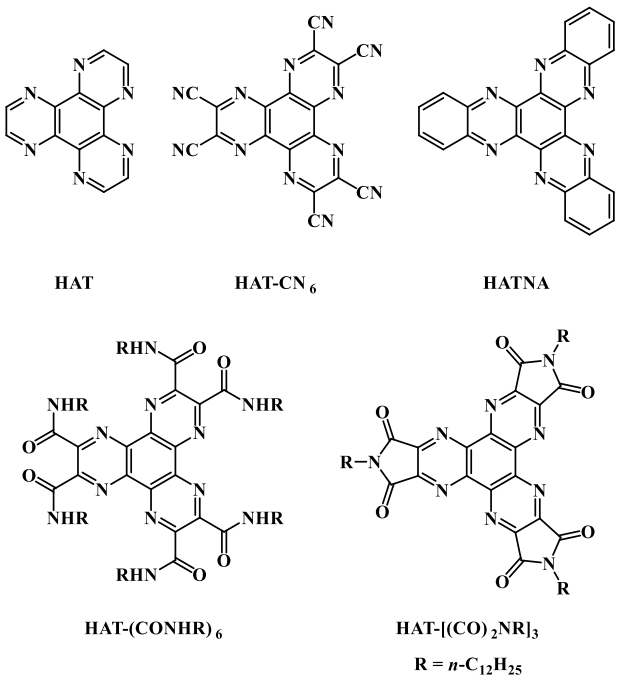

Figure 5.2 Structures of 1,4,5,8,9,12-hexaazatriphenylene (**HAT**)[9] and its derivatives; **HAT-CN6**,[9] **HATNA**,[9] **HAT-(CONHR)6**[12] **and HAT-[(CO)2NR]3**[24]

Recently, **HAT** and its extended derivatives have been demonstrated as good n-type semiconducting materials.[12,19,25] These HAT-based materials, when properly substituted, show self-assembling behaviour both in solution and bulk state to form

one-dimensional columnar-type aggregates.[16,19,25,26–28] Though having self-assembling nature, most of these reported large polycyclic aromatic molecules are either showing n-type or p-type semiconducting characteristics.

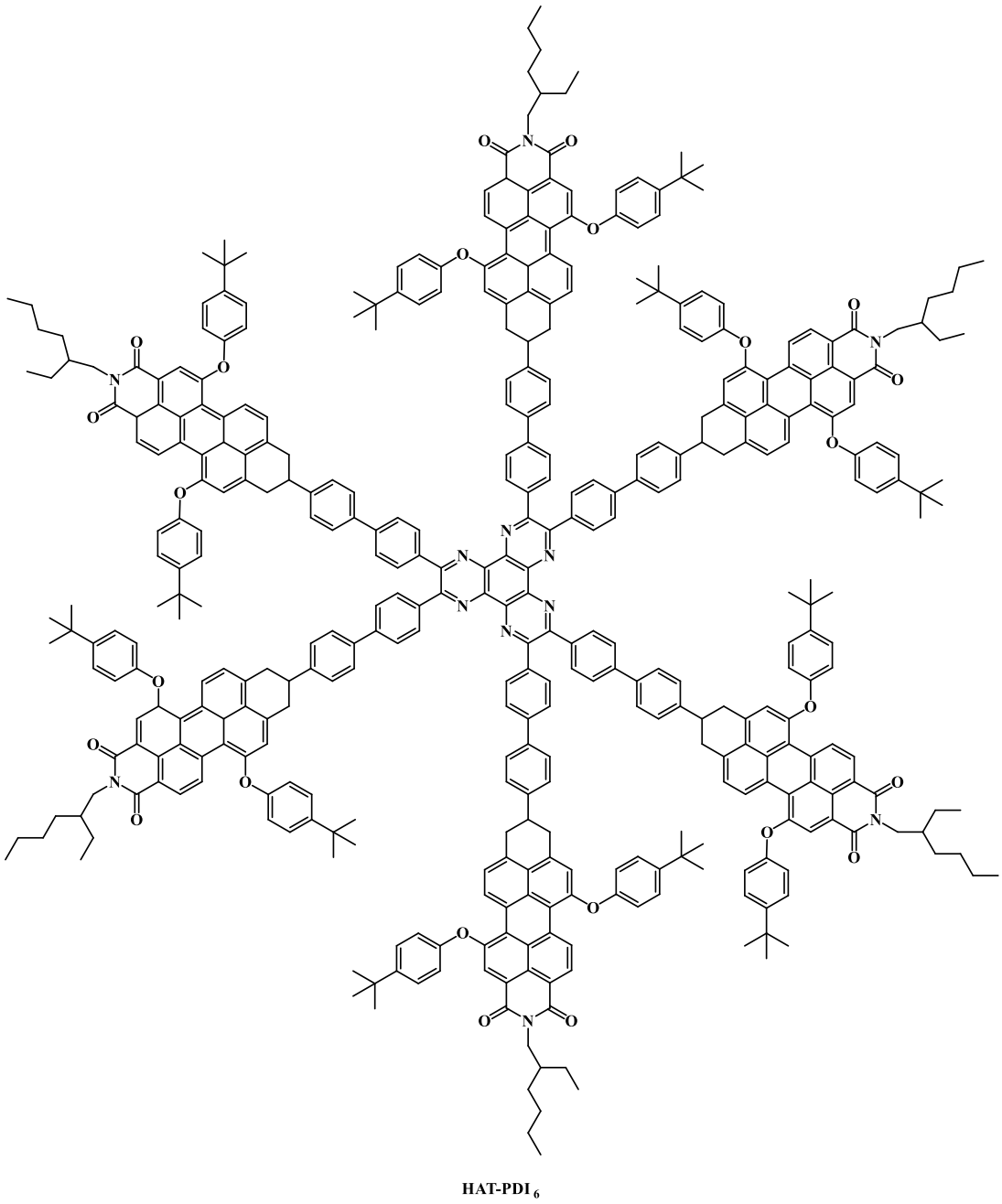

HAT-PDI $_6$

Figure 5.3 Perylene diimide-appended HAT-derivative (**HAT-PDI$_6$**)[26]

Ishi-i *et al*. reported light harvesting and energy-transfer system, **HAT-PDI$_6$**, containing six perylene diimide appended hexaazatriphenylene (HAT), which can self-assemble to form a stable dimer aggregate in both solution and film state (Figure 5.3). In the aggregate structure, an efficient energy transfer from the HAT-core to the

peripheral PDI moiety takes place, which was easily visualized by change in the emission colour from green HAT emission to red PDI emission.[26]

Ishi-i *et al*. reported another hexaazatriphenylene (HAT)-based fused system, **HAT-(phen)$_3$-C$_{12}$**, having a large aromatic core which can exhibit n-type semiconducting behaviour owing to the high electron affinity resulting from the central HAT-core and three peripheral phenanthrolino (phen) moieties (Figure 5.4). This system exhibits self-assembling behaviour in both solution and film state and these extended aggregates of the π-staked aromatic moieties can provide an efficient path for electron-carrier transport within the aggregate structures.[19] Recently, Wang *et al*. reported hexaazatriphenylene derivative, **HAT-Py$_3$**, containing three fused pyrazine units fused with central HAT-core (Figure 5.4). The synthesized **HAT-Py$_3$** exhibited significantly lowered LUMO energy levels of −4.02 eV (even lower than the well-known n-type material PCBM), due to the presence of strong electron withdrawing pyrazine units (Py) fused with HAT-core.[27]

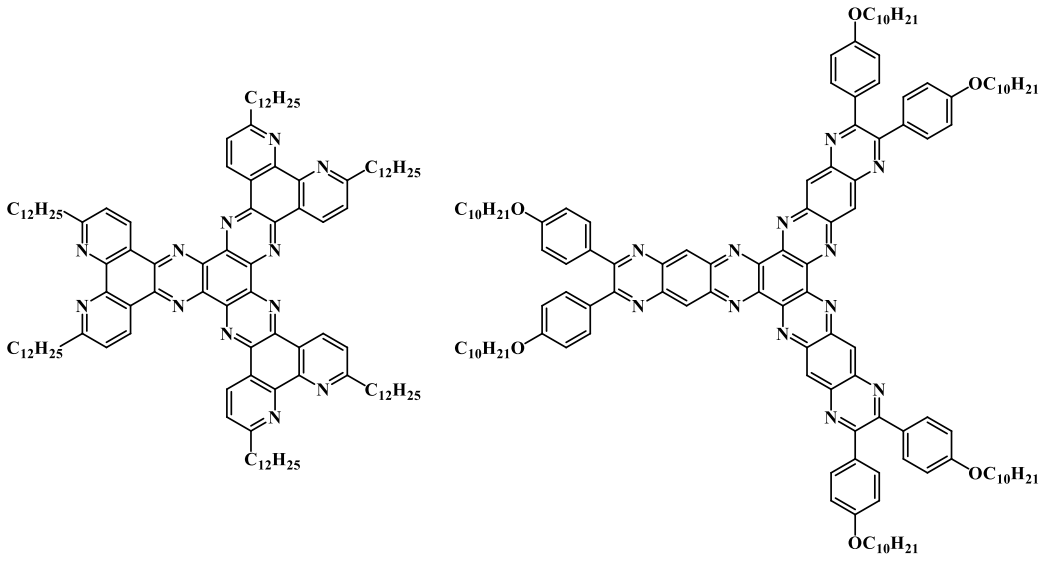

Figure 5.4 Structures of some reported n-type HAT-based molecules (**HAT-(phen)$_3$-C$_{12}$**[19] and **HAT-Py$_3$**[27])

The construction of electron donor-acceptor ensembles, capable of transporting electrons and holes at the same time is important for their application in organic field effect transistors (OFETs) and organic light emitting field effect transistors (OLETs).[8,29,30] The charge transfer complexes containing alternating donor-acceptor stacks exhibit high order geometry.[31] The prime requirement for building highly

ordered donor-acceptor assemblies is strong interaction between electron donor-acceptor pairs as a result of complementary electronic characters. Such well-known pairs are bipyridinium[31] or aromatic diimide[32–36] as acceptors and dioxyarenes[32–39] or tetrathiafulvalene[37,39–42] (TTF) as donors.

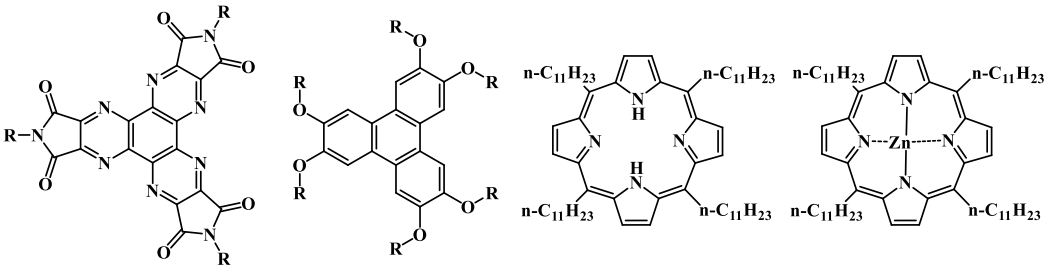

Figure 5.5 Structures of some donor-acceptor pairs which are capable of forming charge transfer π-complexes

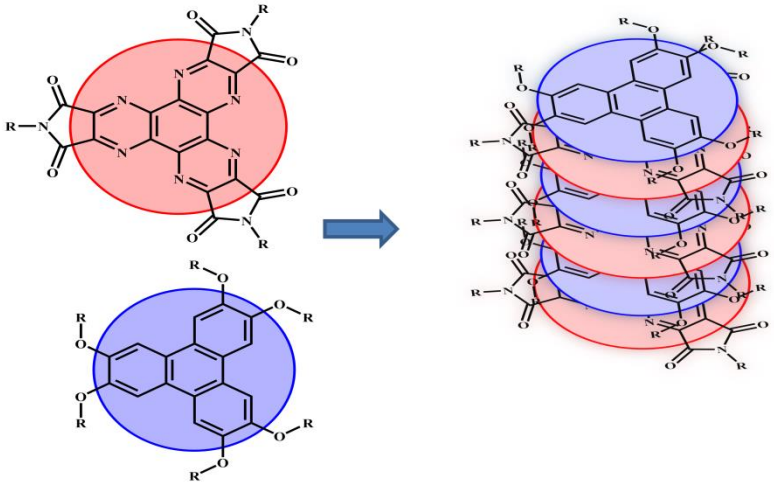

Figure 5.6 Formation of charge transfer π-complex using **HAT-TIm-C12** (acceptor) and **TP-C12** (donor)

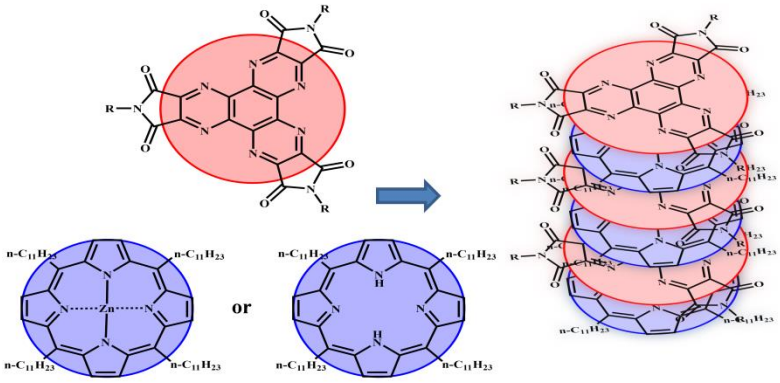

Figure 5.7 Formation of charge transfer π-complex using **HAT-TIm-C3** (acceptor) and **H2-P** or **Zn-P** (donors)

Klivansky *et al.* have reported one of such highly ordered donor-acceptor (D-A)

assembly using HAT-tris(imide), **HAT-TIm-C$_{12}$** as an electron acceptor and hexaalkoxytriphenylene, **TP-C$_{12}$** as electron donor utilizing the π–π interaction between D-A pairs (Figure 5.5 and 5.6).[25] Aoki *et al*. reported formation of face-to-face 1:1 charge transfer π-complexes between HAT-tris(imide), **HAT-TIm-C$_3$** and porphyrin derivatives, **H$_2$-P** and **Zn-P**, which are capable of undergoing ultrafast photoinduced electron transfer. These type of charge transfer π-complexes contribute to the highly ordered patterning even in the film state (Figure 5.5 and 5.7).[24] However, regardless of the advances in these self-assembly systems, breakthroughs in new materials development are largely limited by the scarcity of the strongly interacting donor-acceptor pairs.[25]

An alternate approach to this is to construct D-A systems by electron-rich groups conjugated with electron deficient groups, which can self-assemble into columns, thereby forming a single molecule that is proficient of showing both n-type and p-type behaviour. One of these types of D-A systems has recently been reported by Blas-Ferrando *et al.*,[16] in which large star-shaped D-A system **HAT-(ZnPc)$_3$** has been synthesized utilizing the n-type hexaazatriphenylene group fused with three p-type phthalocyanine units and this system exhibits a strong tendency to aggregate both in solution and in bulk (Figure 5.8).[16]

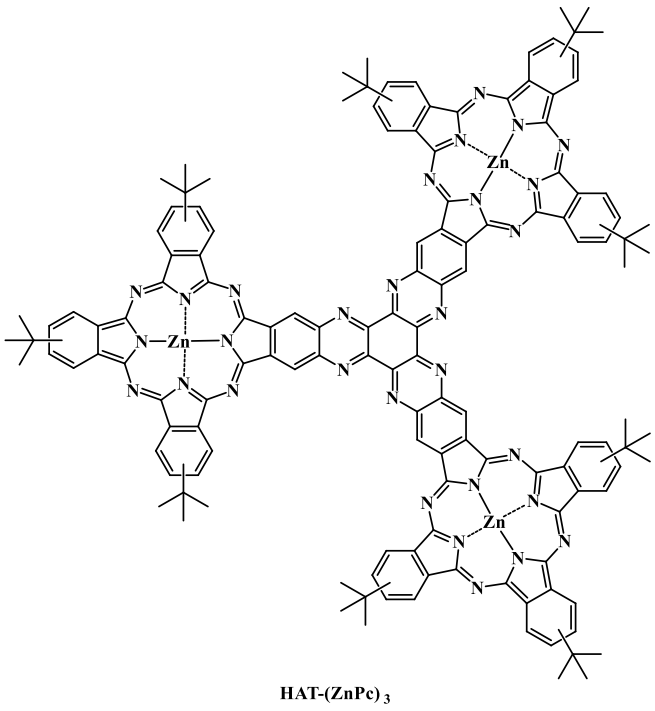

Figure 5.8 Structure of fused donor-acceptor-type molecule, **HAT-(ZnPc)$_3$** having HAT-core

We have developed a new C_3-symmetric covalently linked donor-acceptor-type molecule in which the n-type hexaazatriphenylene core has been fused with three p-type di-amino-di-alkoxybenzene moieties by imidazolo-pyrrolone type linkage, forming a 13 fused ring system, **HAT-IPN** (Figure 5.9). Synthesized molecule shows ambipolar behaviour as well as strong self-assembling nature, forming one-dimensional aggregates.[43]

Results and discussion

Synthesis of hexaazatriphenylene core containing molecule HAT-IPN

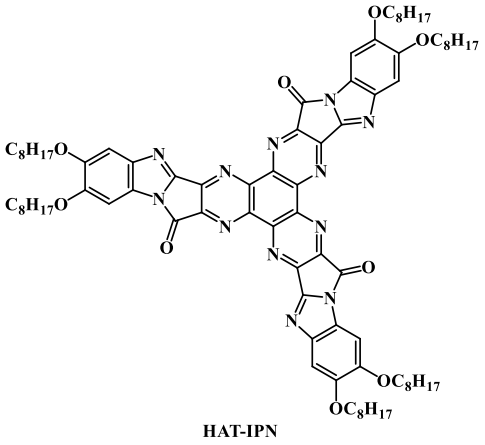

Figure 5.9 Structure of C_3-symmetric donor-acceptor type molecule **HAT-IPN**[43]

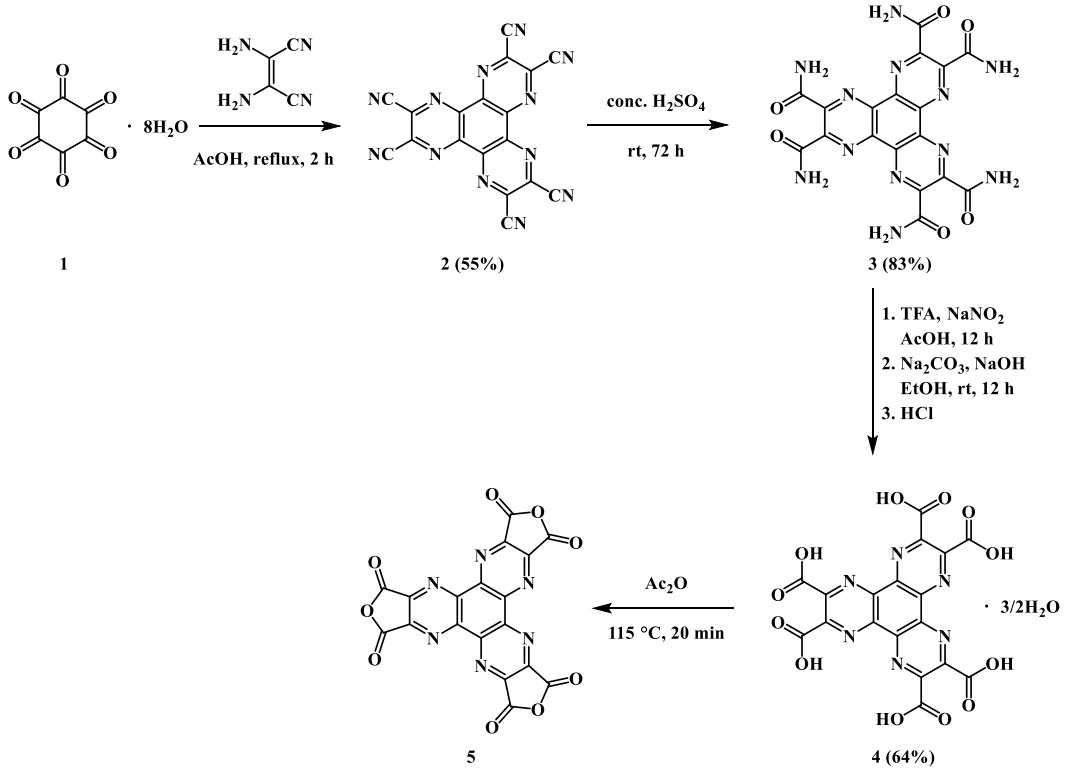

Scheme 5.1 Synthesis of compound **5** (HAT-trisanhydride)

HAT-IPN with six *n*-octyloxy groups was synthesized by the condensation-cyclisation reaction of corresponding hexaazatriphenylenehexacarboxylic acid trisanhydride **5** with 4,5-diamino-1,2-dioctyloxybenzene **10** (Scheme 5.1). The compound **5** was synthesized according to the procedure reported by Kanakarajan *et al.*[44] (Scheme 5.1) and compound **10** was synthesized according to the literature procedure reported by Nagarjuna *et al.*[45] (Scheme 5.2).

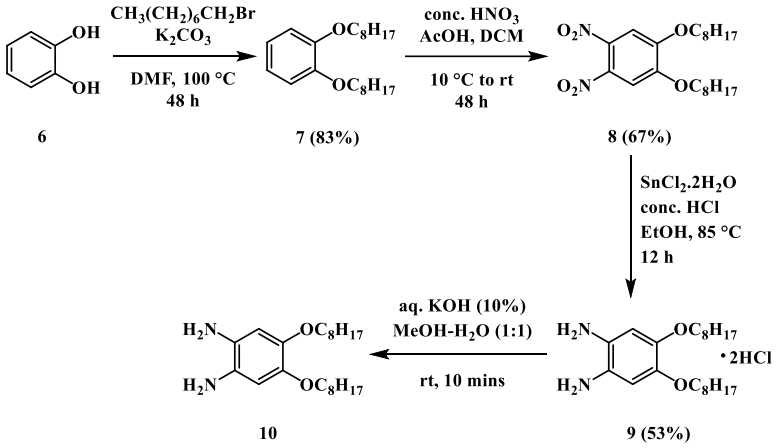

Scheme 5.2 Synthesis of compound **10** (4,5-diamino-1,2-dioctyloxybenzene)

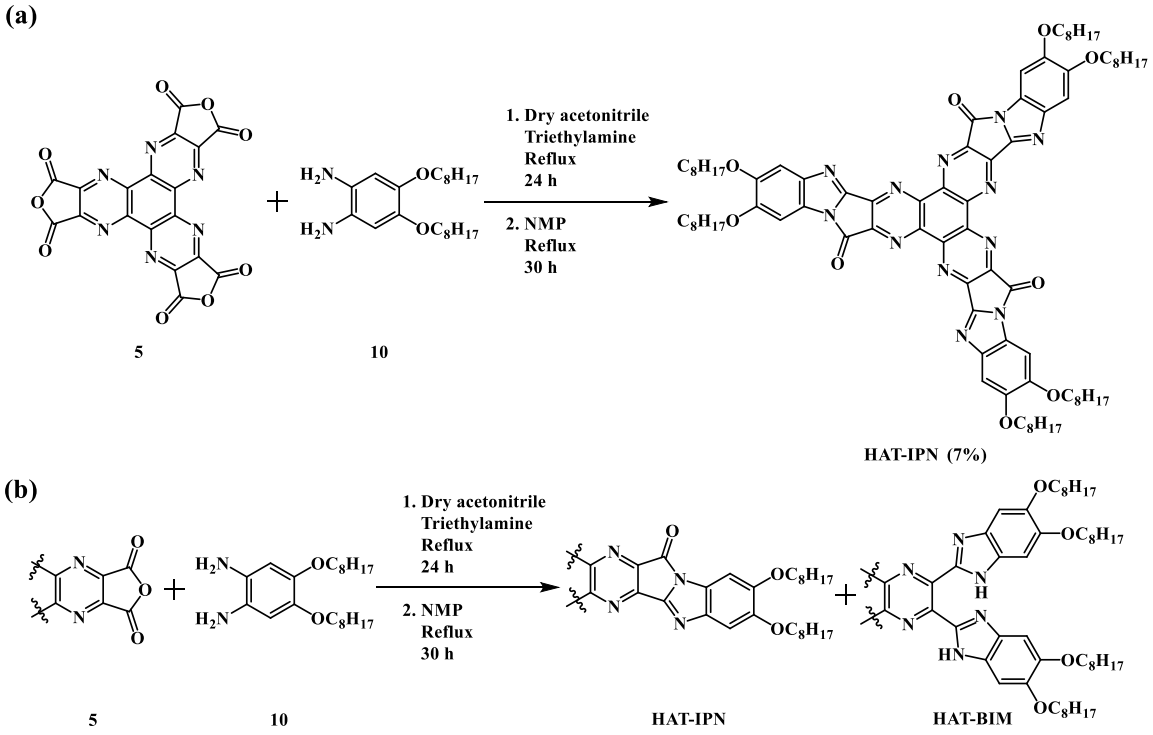

Scheme 5.3 (a) Synthesis of **HAT-IPN** from HAT-trisanhydride **5** (1 eq.) and 4,5-diamino-1,2-dioctyloxybenzene **10** (4.5 eq.); (b) The effect of stoichiometric ratio of starting materials over the side product (**HAT-BIM**) formation[43]

Both the starting materials required for the synthesis of **HAT-IPN** being unstable and moisture sensitive were used as prepared without any purification

attempts. The condensation reaction between anhydride and diamine was carried out in refluxing dry acetonitrile using triethylamine as a base. The resulting condensation product was isolated by removing the solvent under high vacuum and carried forward to the cyclisation step by dissolving the crude condensation product in *N*-methylpyrrolidine-2-one (NMP) and refluxing the resulting reaction mixture for 30 h. The crude product **HAT-IPN** was extracted using ethyl acetate and was purified by column chromatography over silica gel. The stoichiometric ratio of starting materials also plays a key role in the synthesis of **HAT-IPN**. Ideally, the stoichiometric ratio of 1:3 (compound **5**: compound **10**) is required for the synthesis of **HAT-IPN**, but due to the possibility of aerial oxidation of diamine, a slight excess of compound **10** (4.5 eq.) was taken. On the other hand, excessive diamine (> 4.5 eq.) would lead to the formation of bisbenzimidazole (**HAT-BIM**) instead of imidazolo-pyrrolone (**HAT-IPN**). Also, **HAT-IPN** formed in the reaction mixture can also react with 4,5-diamino-1,2-dioctyloxybenzene to give bisbenzimidazole, even at lower temperatures. The formation of the side products in the synthesis of **HAT-IPN** can be related to the strain in the imidazolo-pyrrolone structure of **HAT-IPN**.[38] Similarly, lesser diamine (< 3.0 eq.) would lead to the formation of mono- and di- imidazolo-pyrrolone products. The lower isolated yield of **HAT-IPN** (7%) can be justified by the instability of the starting materials (HAT-trisanhydride, **5** and 4,5-diamino-1,2-dioctyloxybenzene, **10**), decomposition products of the starting materials as well as the possible formation of the side products.

The synthesized **HAT-IPN** was characterized by ^{1}H and ^{13}C NMR and elemental analysis. ^{1}H NMR spectrum of **HAT-IPN** showed a single peak at 7.05 ppm corresponding to the aromatic proton and the rest of the signals correspond to the *n*-octyl chain protons. In ^{13}C NMR spectrum of **HAT-IPN**, carbonyl carbon of pyrrolone ring (−N=C−*C*(=O)−N−) appears at 173.2 ppm. The imidazole ring bridge-head carbon is at 152.2 ppm (−C(=O)−N−*C*=N−) and the inner aromatic ring carbon of hexaazatriphenylene core (=N−*C*=*C*−N=) appears at 131.0 ppm. The outer aromatic ring carbon (−O−*C*=CH−) appear at 147.2 ppm and outer ring carbon of hexaazatriphenylene core (−N=*C*−C=N−) appear at 130.0 ppm due to the fused pyrrolidinone ring attached to it, while the outer benzimidazole ring carbons appear at 132.4, 128.2, 126.5 and 99.7 ppm, respectively. Rest of the signals correspond to the

carbons of the *n*-octyloxy group. The one-dimensional π-stacking of **HAT-IPN** was evidenced by ^{13}C NMR spectroscopy (See Figure 5.10a, b and c).

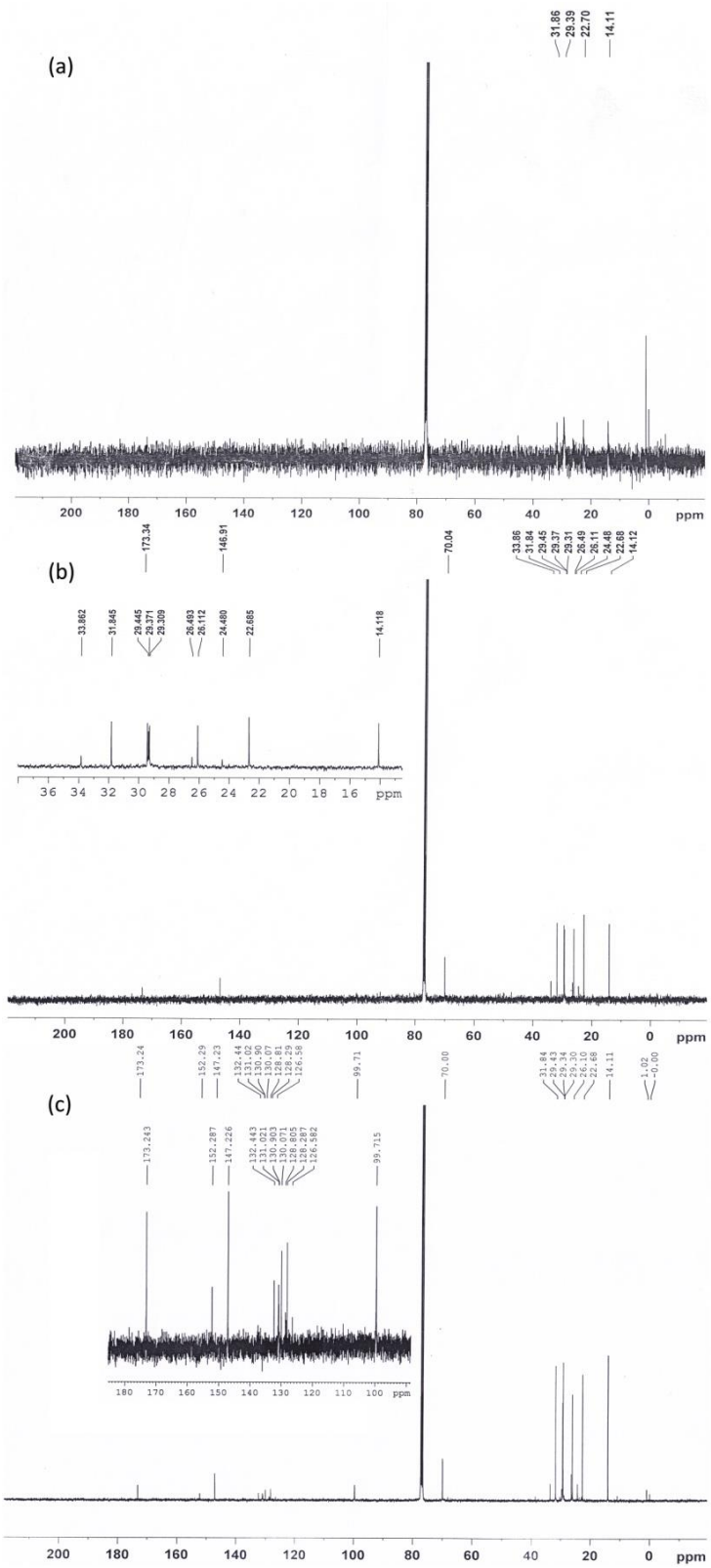

Figure 5.10 ^{13}C NMR of **HAT-IPN** ($CDCl_3$) recorded at different delay time (D1) and scan rate (NS), exhibiting one-dimensional π-stacking; (a) D1 2 sec, NS 1024 (b) D1 5 sec, NS 1024 and (c) D1 5 sec, NS 6144.

Because of the one-dimensional π-π stacking of the **HAT-IPN** molecules in $CDCl_3$, it behaves as a physical polymer rather than behaving as individual molecules, owing to which the relaxation time (delay time D1) required for the magnetic vector of ^{13}C nuclei is higher. Thus, the complete ^{13}C NMR spectrum of **HAT-IPN** with all corresponding carbon signals was obtained by increasing the number of scans from 1024 to 6144 and given delay time D1 of 5.00 seconds.

Photo physical properties and dynamic light scattering studies

The UV-visible absorption spectrum of **HAT-IPN** exhibits absorption resulting from the monomers as well as from the aggregates as shown in Figure 5.11a.

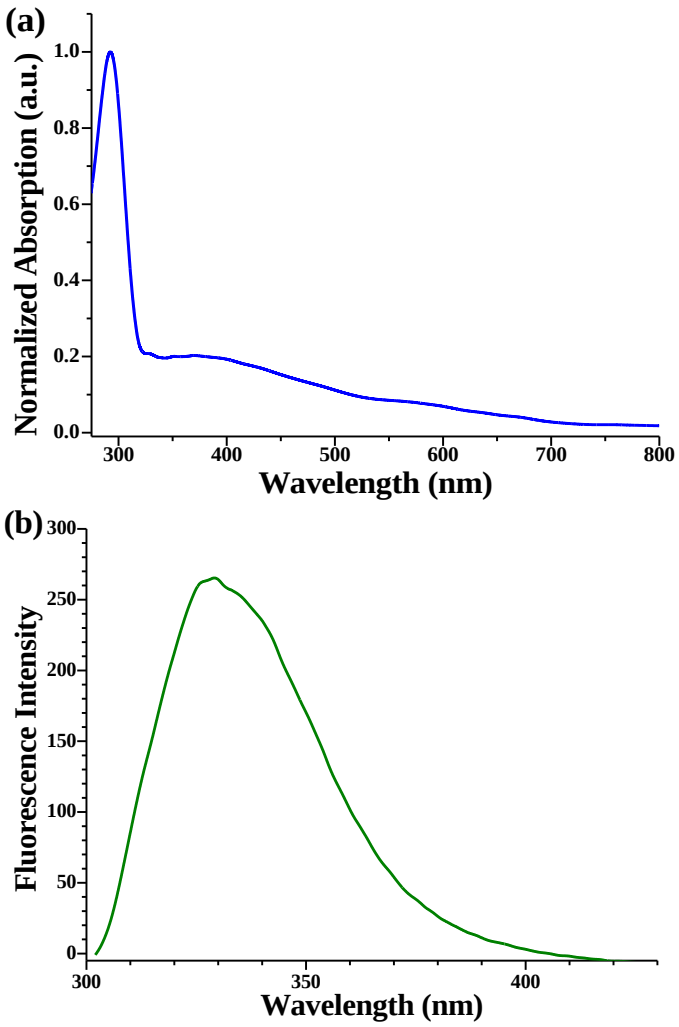

Figure 5.11 (a) UV-visible spectrum of **HAT-IPN** in methanol (1.2 ppm); (b) Fluorescence spectrum of **HAT-IPN** in methanol excited at 292 nm

The UV-visible spectrum of **HAT-IPN** in methanol exhibited two absorption bands; the first band at 292 nm and the second broad structured band ranging from 320 nm to 700 nm. The second lower energy absorption band is broadened and the intensity

of the band is much lowered because of the strong aggregation.[16,38] On the other hand, the intensity of the first absorption band at 292 nm, which corresponds to the π–π* transitions is greatly enhanced because of the formation of π-stacked aggregates.[38] The steady-state fluorescence spectrum of **HAT-IPN** in methanol (Figure 5.11b) showed emission at 330 nm when excited at 292 nm by a single monochromatic beam. The emission spectrum showed combined emission from both the molecules and aggregates, as suggested by the broadening of the emission peak. The relative fluorescence emission quantum yield of **HAT-IPN** in methanol is measured to be 23.1% with the reference of quinine sulfate (54%) in 0.01 M H_2SO_4 solution.

The dynamic light scattering (DLS) study revealed self-aggregating nature of **HAT-IPN** in the solution phase. **HAT-IPN**, having a central hexaazatriphenylene moiety, is a disc-shaped flat molecule with an extended π-conjugation. These disc-shaped molecules having a large aromatic core exhibit self-assembling tendency both in solution and in film state, owing to the strong π–π interaction between the large aromatic core.[16,19,25,38] The dynamic light scattering (DLS) study of **HAT-IPN** solution in methanol (250 ppm) showed the effective diameter of 364 nm, which indicates that small sized π-stacked aggregates are already been formed because of the strong π–π interactions between the **HAT-IPN** molecules. Upon seven-fold dilution of this solution, almost five-fold increase in the effective diameter of the aggregates is observed, ranging from 364 nm to 1870 nm, which can be ascribed to the formation of larger π-extended aggregates from the smaller aggregates (see Figure 5.12). These aggregates having wide π-face overlap exhibits promising electron-hole transport along the π-stacked aggregate structure.[19]

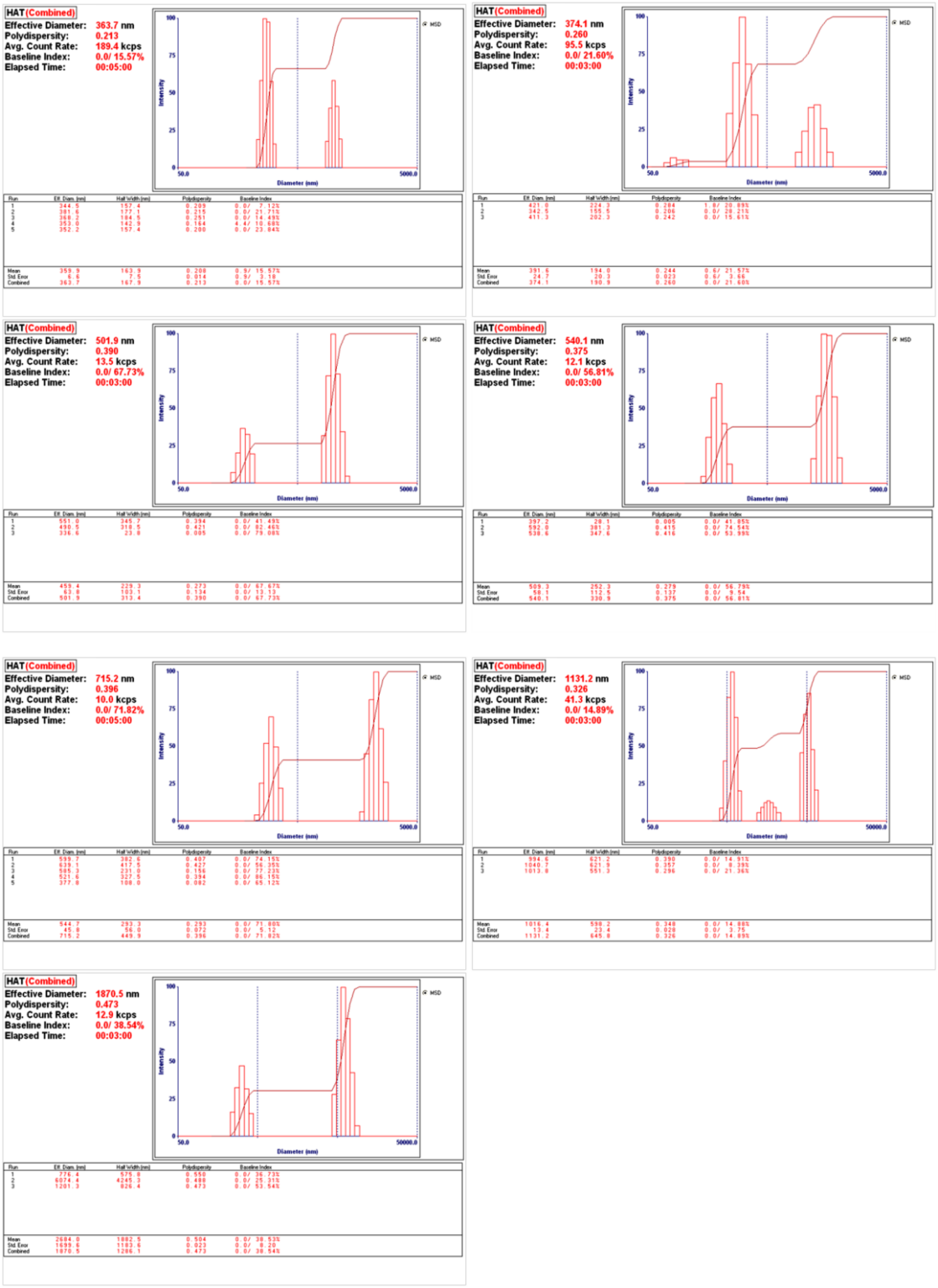

Figure 5.12 DLS data of **HAT-IPN** solution in methanol showing increase in size of aggregates up on dilution

Electrochemistry of HAT-IPN

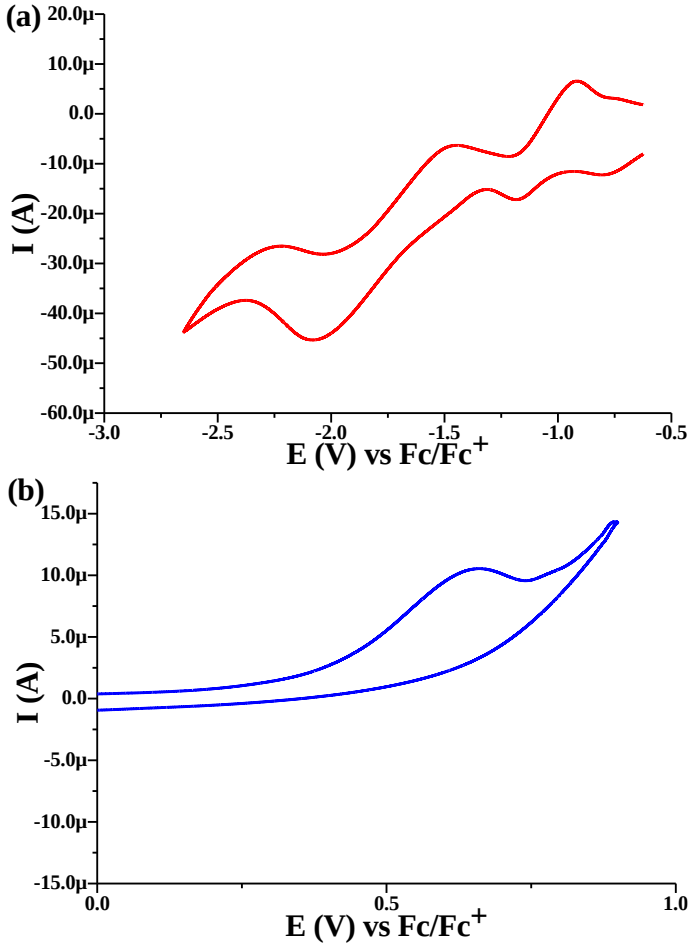

Figure 5.13 (a) Reduction wave and (b) oxidation wave of HAT-IPN in THF using $TBAPF_6$ as supporting electrolyte at scan rate of 100 mV/s, using cyclic-voltammetry

The ambipolar (D-A) character and electrochemical stability of **HAT-IPN** were confirmed by cyclic-voltammetry. Cyclic-voltammogram of **HAT-IPN** was recorded using three electrode system: Pt-disc electrode as working electrode, Pt wire as a counter electrode and Ag/Ag^+ as a reference electrode. As shown in Figure 5.13a, three separate reduction peaks were observed at −0.77 V, −1.17 V and −2.05 V versus Fc/Fc^+, corresponding to the n-type HAT core in tetrahydrofuran using tetra-*n*-butylammonium hexafluorophosphate ($TBAPF_6$) as a supporting electrolyte when scanned at a scan rate of 100 mV/s. On the other hand, one oxidation peak was observed at +0.64 V corresponding to the three outer p-type dialkoxybenzoimidazole moieties (Figure 5.13b). The frontier orbital energy levels of **HAT-IPN** were calculated using the first oxidation peak (E_{oxi}) and first reduction peak (E_{red}). The values of E_{HOMO} and E_{LUMO} were calculated using the equations: $E_{HOMO} = -(E_{oxi} + 4.8)$ and $E_{LUMO} = -$

(E_{red} + 4.8). The LUMO energy level of **HAT-IPN** was found to be −4.03 eV. The low lying LUMO level of **HAT-IPN** can be attributed to the presence of acceptor type HAT-core and the fused imidazolo-pyrrolone type structure. Donor-acceptor nature of **HAT-IPN** is also evident from DFT calculated frontier orbitals. LUMOs are mainly located in the central HAT core, whereas the HOMOs have contributions largely coming from the peripheral dialkoxybenzoimidazole part (Figure 5.14).

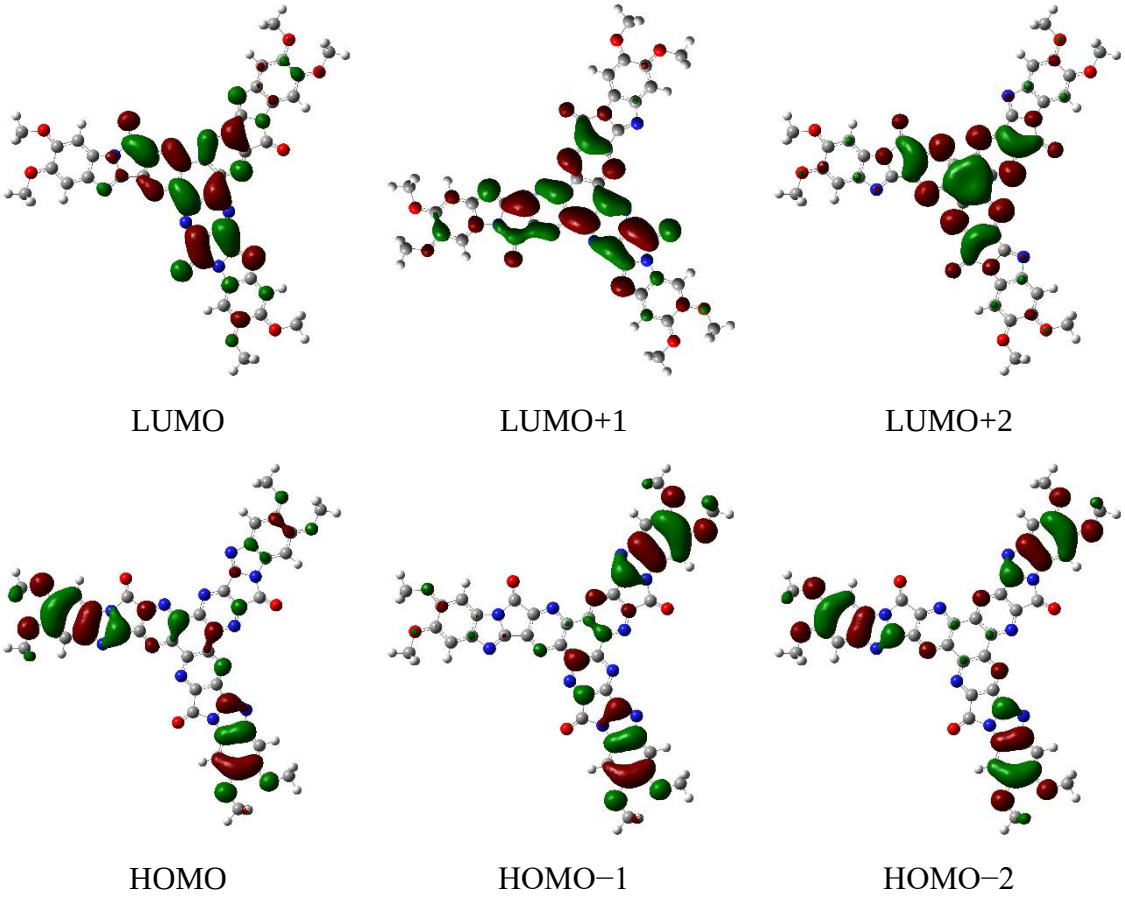

Figure 5.14 Molecular orbital topologies of HAT-IPN calculated at DFT//B3LYP/6-31G(d)[46]

The LUMO and HOMO energy levels of **HAT-IPN** were compared with the HOMO-LUMO levels of other HAT-derivatives reported in the literature (Figure 5.15).

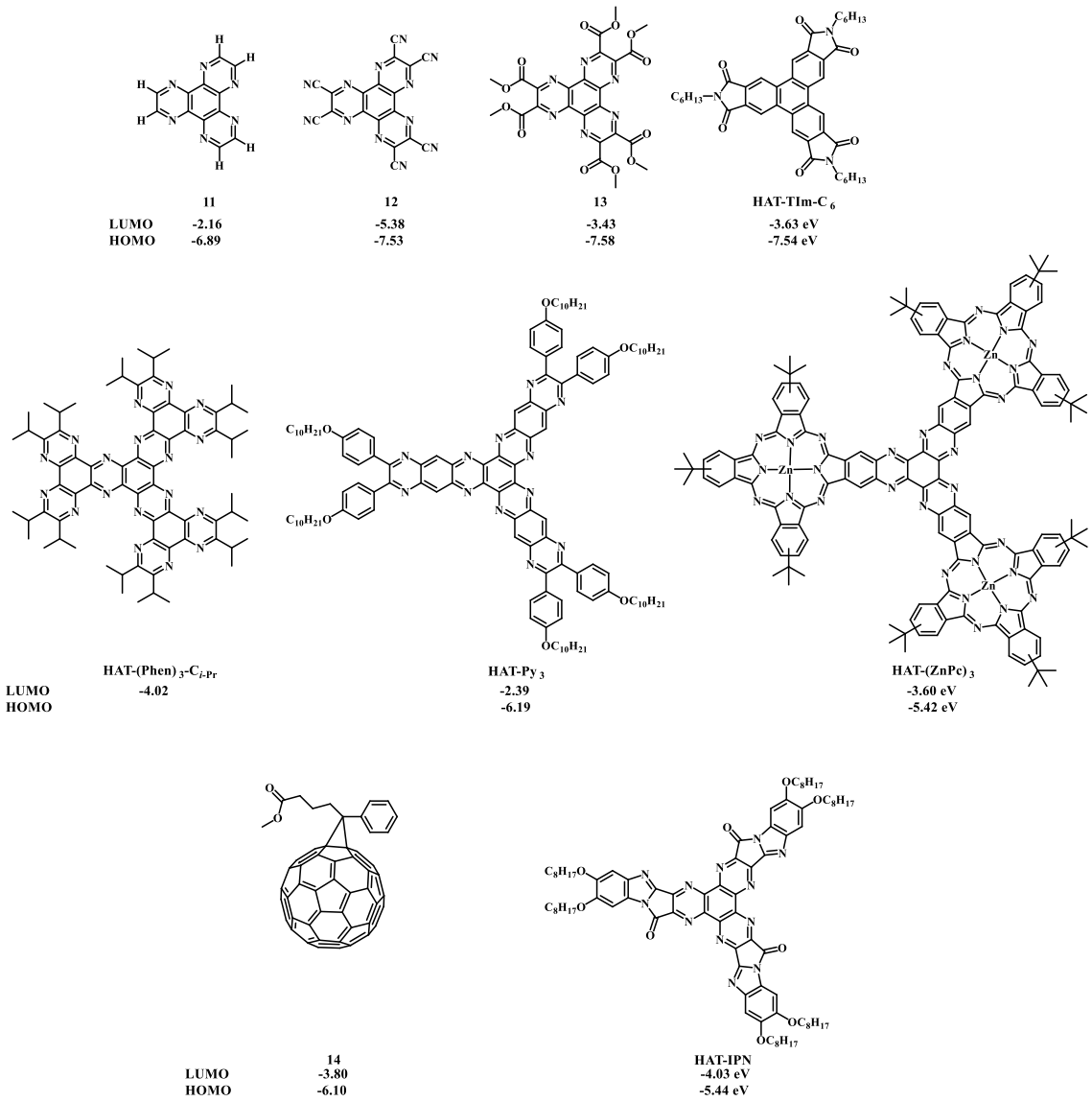

Figure 5.15 Comparison of HOMO and LUMO energy level of **HAT-IPN** with that of some reported HAT-derivatives; **11**[24], **12**[47], **13**[24], **HAT-TIm-C6**[24], **HAT-(Phen)3-C*i*-Pr**[19], **HAT-Py3**[27], **HAT-(ZnPc)3**[16] and **14**[27]

Thermogravimetric analysis, differential scanning calorimetry and atomic force microscopy of HAT-IPN

The HAT-derivative, having alternate three cyano groups and three hexyloxy groups, attached on the periphery of HAT-core as well as the donor-acceptor charge transfer complex made from the HAT-triimide and hexaalkoxytriphenylene exhibit columnar discotic liquid crystalline phase[25,48] which shows that HAT-core having flat-disc like structure, with flexible alkoxy/alkyl side chains may display the presence of columnar discotic mesophase while heating and/or cooling. The thermal behaviour of **HAT-IPN** was characterized by thermo-gravimetric analysis (TGA) as well as differential scanning calorimetry (DSC) (Figure 5.16a and b).

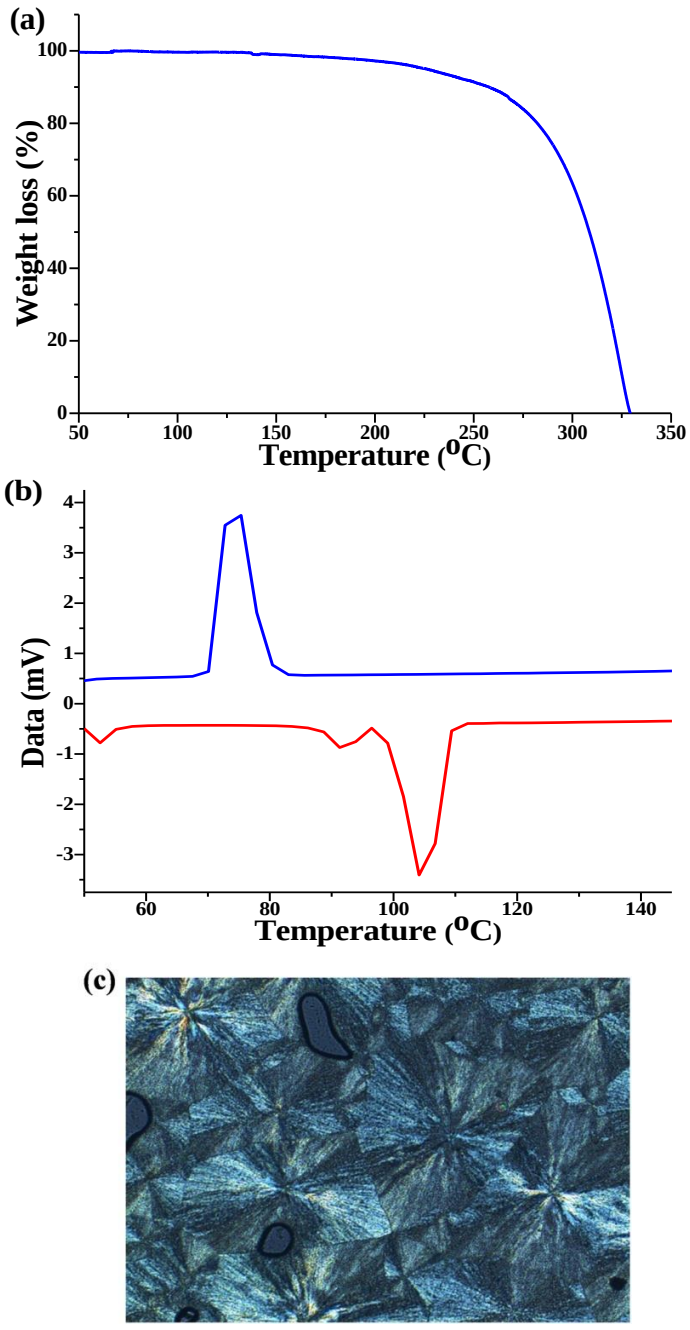

Figure 5.16 Thermal behaviour of **HAT-IPN**; (a) thermogravimetric analysis (TGA) and (b) differential scanning calorimetry (DSC): heating cycle is showed by red line and cooling cycle is showed by blue line. Scan rate is 10 °C/min for both TGA and DSC. N_2 is used as inert gas

Thermogravimetric analysis of **HAT-IPN** (Figure 5.16a) revealed that the molecule is stable up to 225 °C. The DSC analysis of **HAT-IPN** (Figure 5.16b) showed the presence of the mesophase with the endothermic peak at 91.3 °C in the heating cycle, followed by the endothermic peak at 104.4 °C which can be correlated to the phase transition of **HAT-IPN** from crystalline solid to isotropic liquid. Upon cooling, the exothermic peak corresponding to the phase transition from isotropic liquid to the

crystalline solid appears at 75.3 ºC. The corresponding polarizing optical microscope (POM) images indicating the phase transition during heating couldn't be captured, however, POM images showed that upon cooling from the isotropic liquid, **HAT-IPN** crystallized out in focal conic texture, showing cog-wheel type arrangement (Figure 5.16c).

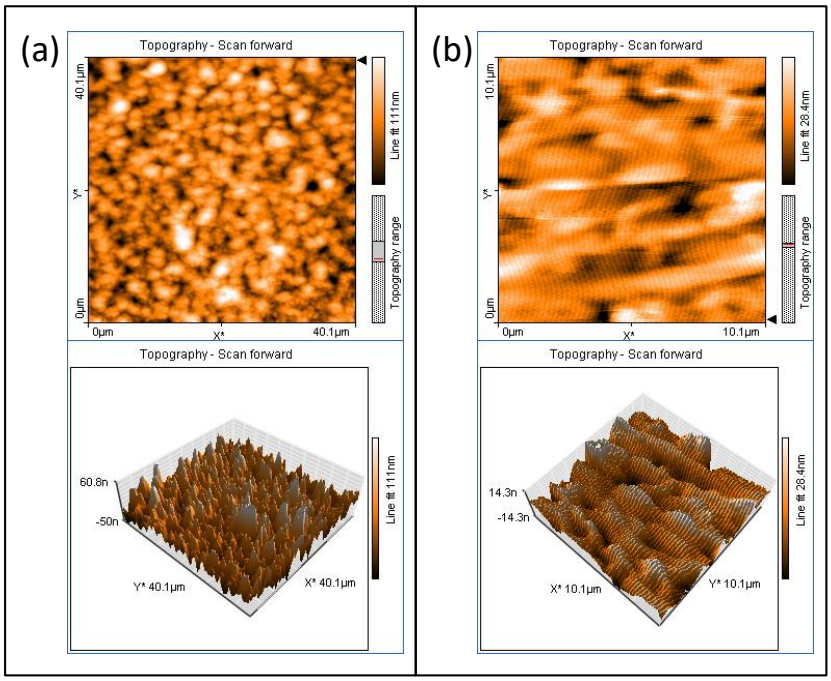

Figure 5.17 AFM images of **HAT-IPN** film; (a) after annealing with chloroform vapours and (b) non-annealed film

The formation of the π-stacked aggregate structure of **HAT-IPN** was also evidenced by atomic force microscopy (AFM) observation. AFM image of chloroform solution cast film after annealing with chloroform vapours (Figure 5.17a) indicates the π-stacked self-assembled aggregates in form of the cone-shaped structures[49] that average 70-80 nm in height and 100-150 nm in base width. Moreover, the AFM image of the non-annealed film of **HAT-IPN** (Figure 5.17b) did not exhibit any cone-shaped structures, instead of that layered structure was observed which indicated that the formation of π-stacked aggregates takes place only after annealing with solvent vapours.

Conclusion

A self-assembling C_3-symmetric covalently linked donor−acceptor-type molecule, hexaazatriphenylene-tris(dialkoxybenzimidazolo-pyrrolone) (HAT-IPN) is synthesized for the first time utilizing triple condensation-cyclization approach between HAT-

trisanhydride and 4,5-diamino-1,2-dioctyloxybenzene. The ambipolar behaviour of **HAT-IPN** is confirmed by cyclic-voltammetry. Moreover, the self-assembling tendency of the **HAT-IPN** is evidenced by the ^{13}C NMR spectroscopy, dynamic light scattering, differential scanning calorimetry and atomic force microscopy, indicating the formation of one-dimensional π-stacked aggregates. An efficient electron-hole transport could be achieved within the structure of these extended aggregates.[12,19,25]

Experimental procedures

General procedures

All the chemicals were reagent grade and used as purchased. Moisture-sensitive reactions were performed under an inert atmosphere of dry nitrogen with dried solvents. Reactions were monitored by thin-layer analysis (TLC) analysis using Merck 60 F_{254} aluminium-coated plates and the spots were visualized under ultraviolet (UV) light. Column chromatography was carried out on silica gel (60–120 mesh). Mass spectra were recorded on Thermo-Fischer DSQ II GCMS instrument. NMR spectra were recorded on a Bruker Avance-III 400 spectrometer in $CDCl_3$ and DMSO-D_6. UV-Visible absorption spectra were recorded on Jasco V-630 spectrophotometer using quartz cuvette. The steady-state fluorescence spectra were recorded on Jasco FP 6300 spectrofluorometer using quartz cuvette. CV data were obtained with CH Instruments model of CHI 600C with three electrode (Pt disc/glassy carbon as the working electrode, platinum wire as the counter electrode, and non-aqueous $Ag/AgNO_3$ as the reference electrode) cells in anhydrous THF solution containing 50 mM tetra-*n*-butylammonium hexafluorophosphate at a scan rate of 100 mV/s under an N_2 atmosphere. Thermo-Gravimetric Analysis (TGA) of the polymer was done on Exstar SII TG/DTA 6300 using N_2 as an inert gas. Differential Scanning Calorimetry (DSC) of the polymer was performed with Mattler Toledo DSC822^e under N_2 atmosphere. Polarizing Optical Microscopy was performed on Leica DM 2500P with variable heat platform. DLS studies were performed on the Brookhaven Instrumentation Corporation made a particle size analyzer, model 90 plus. Elemental analysis was performed on Perkin Elmer C/H/N Analyser, 2400 series II.

Compound **2, 3, 4** and **5** were synthesized according to the procedure reported in the literature.[44]

Synthesis of hexaazatriphenylenehexacarbonitrile, **2**: In a three-necked round bottom flask, hexaketocyclohexane octahydrate, **1** (10.0 g, 32 mmol) and diaminomaleonitrile (26.0 g, 240 mmol) were dissolved in glacial acetic acid (1200 mL). The reaction mixture was refluxed for 2 h after which, the reaction mixture was allowed to cool to 70 ^{o}C. The brown-black reaction mixture was filtered hot, and the precipitates were washed with hot glacial acetic acid (3 X 150 mL). The crude product was allowed to dry under vacuum at 60 ^{o}C. The crude product was subjected to the soxhlet extraction using acetonitrile for 36 h. The solvent was evaporated under vacuum to afford pure product as bright yellow solid.

Hexaazatriphenylenehexacarbonitrile, **2**: Bright yellow solid (6.77 g, 55%); ^{13}C NMR (DMSO-D_6, 100 MHz): 114.1, 135.3, 141.5.

Synthesis of hexaazatriphenylenehexacarboxamide, **3**: In a two-necked round bottom flask compound **2** (4.80 g, 32 mmol) was dissolved in 100 mL of concentrated sulphuric acid. The reaction mixture was stirred for 72 h at room temperature after which, it was added drop-wise to vigorously stirring ice-water mixture. The solid was collected by filtration, washed with water (3 X 100 mL) and acetone (3 X 100 mL), and dried at 60 ^{o}C under vacuum to provide pure product as beige yellow solid.
Hexaazatriphenylenehexacarboxamide, **3**: Beige yellow solid (5.10 g, 83%); ^{13}C NMR (DMSO-D_6, 100 MHz): 141.0, 148.7, 166.3.

Synthesis of hexaazatriphenylenehexacarboxylic acid, **4**: In a two-necked round bottom flask, compound **3** (4.92 g, 10 mmol) was dissolved in 150 mL of trifluoroacetic acid at room temperature. To this stirred solution, sodium nitrite (7.0 g, 90 mmol) was added portion-wise over a period of 15 min, keeping the temperature below 25 ^{o}C by cooling in an ice-water bath. During addition, brisk evolution of gas was noted, and the brown solution changed to an orange brown suspension. Immediately, 150 mL of acetic acid was added and the mixture was stirred for 12 h at room temperature. After completion, the reaction mixture was poured into ice-water and the crude product was collected by filtration. The solid was again dissolved in sodium bicarbonate solution (20 g in 150 mL water) and filtered to remove any insoluble materials. The clear yellow filtrate solution was treated with a cold sodium hydroxide solution (20.0 g in 100 mL water) which caused immediate precipitation of sodium hexaazatriphenylenehexacarboxylate as a yellow solid. The complete

precipitation of the salt was caused by the addition of ethanol (30 mL). The product was filtered, washed with 50% aqueous alcohol (3 X 50 mL).

The obtained sodium hexaazatriphenylenehexacarboxylate was suspended in water (100 mL), heated to 50 ^{o}C, and acidified by adding 100 mL of concentrated HC1. The mixture was heated at 90 ^{o}C for 1 h and filtered. The solid was washed with 10% HC1 solution (3 X 25 mL) and deionized water (2 X 25 mL). The product was dried at 80 ^{o}C under vacuum to give compound **5** as its sesquihydrate.

Hexaazatriphenylenehexacarboxylic acid, **4**: Light yellow solid (3.36 g, 64%); ^{13}C NMR (DMSO-D_6, 100 MHz): 142.7, 148.0, 165.2.

Synthesis of hexaazatriphenylenehexacarboxylic acid trisanhydride, **5**: Compound **5** (HAT-trisanhydride) was synthesized from its synthetic precursor, compound **4** (hexaazatriphenylenehexacarboxylic acid) by heating the suspension of later in acetic anhydride at 115-117 ^{o}C for 15-20 min. The yellow suspension turned into an orange-brown clear solution, after which heating was discontinued and the reaction mixture was allowed to cool at room temperature. The excess of acetic anhydride was removed under vacuum and the crude HAT-trisanhydride thus obtained was subjected to the condensation reaction with 4,5-diamino-1,2-dioctyloxybenzene.

Compound **7**, **8** and **9** were synthesized according to the literature procedure.[45]

Synthesis of 1,2-dioctyloxybenzene, **7**: In a two-necked round bottom flask, 1,2-dihydroxybenzene (15.0 g, 136 mmol) was dissolved in 75 mL of DMF. To this stirred solution, K_2CO_3 (56.5 g, 408 mmol) was added in one portion followed by addition of *n*-octylbromide (59.2 mL, 340 mmol) and resulting suspension was stirred at 100 °C under a nitrogen atmosphere for 48 h. After cooling the mixture to room temperature, 750 mL of water was added and the crude product was extracted with dichloromethane (2 X 75 mL). The combined organic layers were mixed, washed with sodium thiosulphate solution and brine solution and dried over anhydrous sodium sulphate. The solvent was evaporated on rotary evaporator leaving behind residual DMF and *n*-octylbromide, which were removed under high vacuum at 100 ^{o}C. The residue was purified by column chromatography over silica gel using 10% ethyl acetate-petroleum ether as an eluent, affording compound **7** as colourless oil.

1,2-dioctyloxybenzene, **7**: Colourless oil (37.8 g; 83%); ^{1}H NMR ($CDCl_3$, 400 MHz): 6.90 (s, 2H), 3.99-4.02 (t, J = 6.8 Hz, 2H), 1.80-1.87 (m, 2H), 1.44-1.52 (m, 2H), 1.30-1.38 (m, 8H) 0.88-0.92 (t, J = 6.8 Hz, 3H). ESI-MS 334.03 [M+].

Synthesis of 1,2-dinitro-4,5-dioctyloxybenzene, **8**: In a 2 litre two-necked round bottom flask, 420 mL of dichloromethane was mixed with 420 mL of glacial acetic acid. To this, compound **7** (35 g, 104 mmol) was added and resulting solution was allowed to cool to 10 °C. After attaining the temperature, concentrated nitric acid (550 mL, 65%) was added drop wise and the reaction mixture was allowed to warm to room temperature and stirred for 48 h. After completion of the reaction, the reaction mixture was poured into ice-water and the dichloromethane layer was separated. The aqueous phase was again extracted with dichloromethane (2 X 200 mL). The combined organic layers were washed with brine, dried over anhydrous sodium sulphate, and concentrated under vacuum. The crude product was purified by re-crystallisation from ethanol.

1,2-dinitro-4,5-dioctyloxybenzene, **8**: Yellow solid (29.7 g, 67%); ^{1}H NMR ($CDCl_3$, 400 MHz): 7.31 (s, 1H), 4.10-4.13 (t, J = 6.4 Hz, 2H), 1.85-1.92 (m, 2H), 1.46-1.54 (m, 2H), 1.33-1.40 (m, 8H), 0.91-0.94 (t, J = 7.2 Hz, 3H). ESI-MS 424.51 [M+].

Synthesis of 4,5-dioctyloxybenzene-1,2-diaminium chloride, **9**: In a 1 litre two-necked round bottom flask, compound **8** (10.0 g, 23.5 mmol) was charged along with $Sn(II)Cl_2.2H_2O$ (42.5 g, 188.0 mmol), concentrated HCl (140 mL, 35%) and absolute ethanol (350 mL). The reaction mixture was allowed to heat to 85 ^{o}C for 12 h. After completion, the reaction mixture was allowed to cool to room temperature and precipitated solid was filtered, washed with water and cold methanol. The precipitates were allowed to dry under vacuum.

4,5-dioctyloxybenzene-1,2-diaminium chloride, **9**: Off white solid (5.46 g, 53%); ^{1}H NMR ($CDCl_3$+CD_3OD 1:1, 400 MHz): 6.71 (s, 1H), 3.87-3.95 (m, 2H), 1.72-1.77 (m, 2H), 1.20-1.42 (m, 10H), 0.83 (br s, 3H).

Note: The hydrochloride salt being unstable was stored as suspension in diethyl ether and was neutralized to compound **10** just prior to the condensation reaction with HAT-trisanhydride.

For the characterization purpose, *N,N'*-(4,5-dioctyloxy-1,2-phenylene)bistrifluoroacetamide was synthesized from compound **10** using following synthetic procedure. In a two necked round bottom flask, compound **10** (0.100 g, 0.27 mmol) was dissolved in 10 mL of dry THF. To this, trifluoroacetic anhydride (0.1 mL, 0.69 mmol) and triethylamine (0.19 mL, 1.37 mmol) were added drop wise. The resulting reaction mixture was allowed to stir at room temperature for 3 h. After completion, the solvent was evaporated under reduced pressure and the crude product was directly subjected to the column chromatography over silica gel. The pure product was eluted using 30% ethyl acetate-petroleum ether as an eluent.

N,N'-(4,5-dioctyloxy-1,2-phenylene)bistrifluoroacetamide; White solid; ^{1}H NMR ($CDCl_3$, 400 MHz): 8.47 (s, 1H), 6.91 (s, 1H), 3.97-4.00 (m, 2H), 1.80-1.87 (m, 2H), 1.44-1.50 (m, 2H), 1.34-1.38 (m, 8H), 0.91-0.94 (m, 3H).

Compound **10** (1,2-diamino-4,5-dioctyloxybenzene) was synthesized as follow. Compound **9** was dissolved in methanol:chloroform (1:1) and to this solution was added 10% aqueous KOH solution drop-wise. After stirring at room temperature for 15 min, the bulk was extracted multiple times with aliquots of dichloromethane. A combined organic layer was washed with brine and finally with water to remove traces of alkali and evaporated to dryness under vacuum to yield compound **10** as dark yellow to orange solids. The crude product being unstable was forwarded to the next step without any purification.

Synthesis of **HAT-IPN**: HAT-IPN was synthesized using the modification of the literature procedure reported by Xiao *et al*.[50] The crude compound **5** (0.44 g; 1 mmol) was dissolved in dry acetonitrile and kept stirring under nitrogen atmosphere for 5 min at room temperature. Freshly prepared compound **10** (1.64 g; 4.5 mmol) was suspended in dry acetonitrile along with triethylamine (1.39 mL; 10 mmol) and was taken in the pressure equalizing addition funnel. The later was added drop-wise to the stirring mixture of compound **5** in acetonitrile at room temperature under a nitrogen atmosphere. At this point, the colour change of the reaction mixture from orange to red wine was noticed. After complete addition, the reaction mixture was refluxed at 90 ^{o}C under nitrogen atmosphere. After 24 h, heating was discontinued and the reaction mixture was allowed to cool to room temperature. The crude condensation product was obtained by removal of the solvent under reduced pressure, which was carry forwarded to the cyclization reaction without any purification. The crude product was dissolved

again in *N*-methylpyrrolidin-2-one (NMP) (50 mL) and subjected to reflux under a nitrogen atmosphere at 190 ^{o}C. After 30 h, heating was discontinued and the reaction mixture was allowed to attain room temperature. The reaction mixture was quenched with 500 mL of de-ionized water and was extracted using aliquots of ethyl acetate (3X50 mL). The combined organic layer was washed with brine (2X100 mL) and finally with de-ionized water (1X100 mL) for complete removal of NMP. The organic layer was dried over anhydrous sodium sulfate and was evaporated under vacuum. The crude product obtained was subjected to column chromatography over silica gel using 80% ethyl acetate-petroleum ether as eluent. The pure product **HAT-IPN** obtained from the column is a yellowish powder which was further purified by crystallization from methanol-water.

HAT-IPN: Reddish-yellow solid (0.09 g, 7%); ^{1}H NMR ($CDCl_3$, 400 MHz): 7.05 (s, 1H), 3.98−4.01 (t, J = 6.4 Hz, 2H), 1.80−1.86 (m, 2H), 1.46−1.50 (m, 2H), 1.30−1.34 (m, 8H), 0.88−0.91 (m, 3H). ^{13}C NMR ($CDCl_3$, 100 MHz; D1 5 sec, NS 6144): 173.2, 152.3, 147.2, 132.4, 131.0, 130.9, 130.0, 128.8, 128.2, 126.6, 99.7, 70.0, 31.8, 29.4, 29.3, 29.3, 26.1, 22.7, 14.1. Elemental Analysis: % C: 70.59 (70.56); % H: 7.65 (7.61); % N: 11.71 (11.76). Values in parentheses are calculated values.

Spectral data

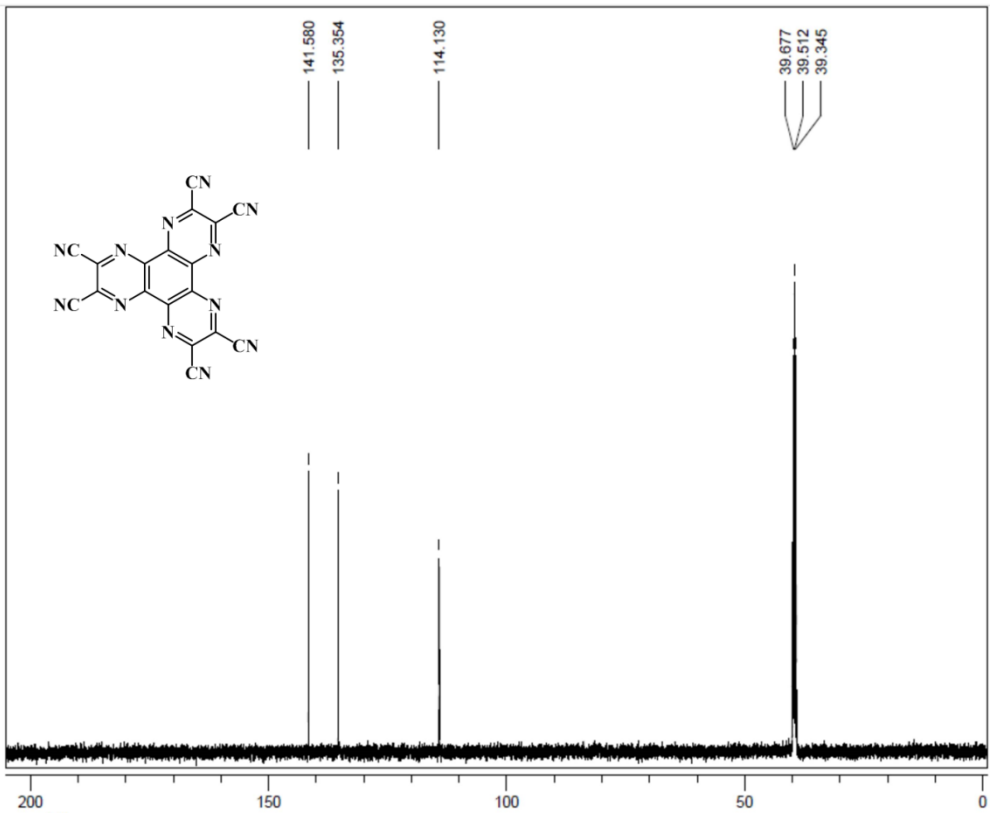

Figure 5.18 ^{13}C NMR spectrum of compound **2**

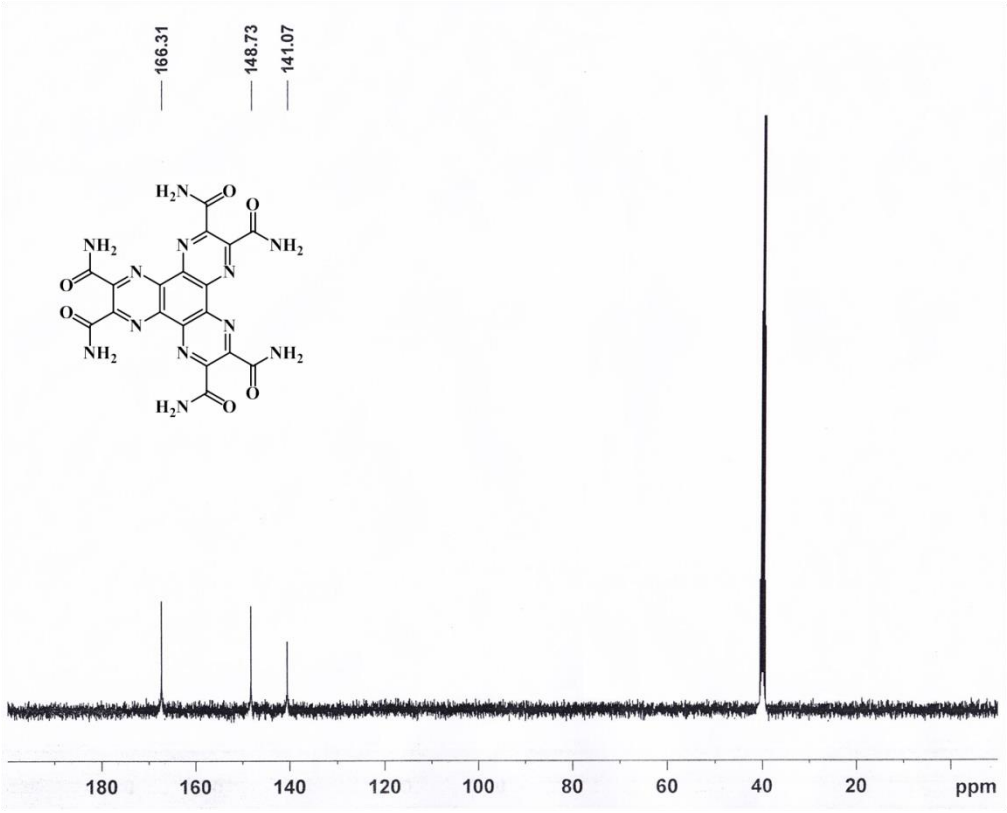

Figure 5.19 ^{13}C NMR spectrum of compound **3**

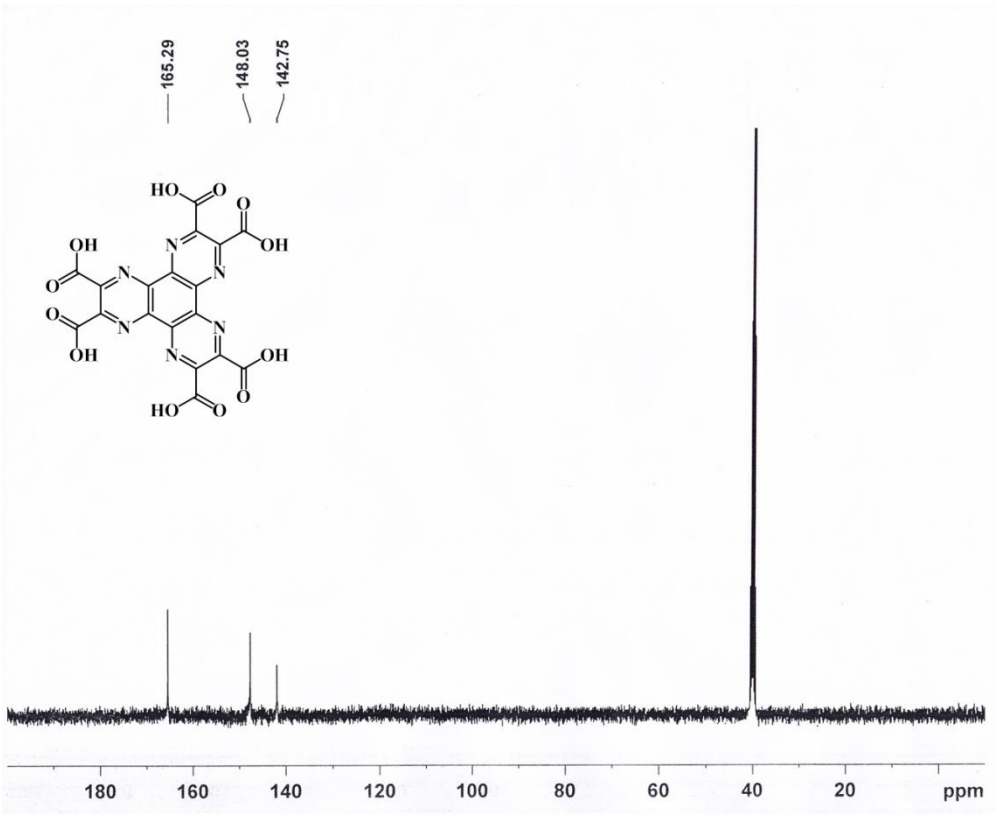

Figure 5.20 ^{13}C NMR spectrum of compound **4**

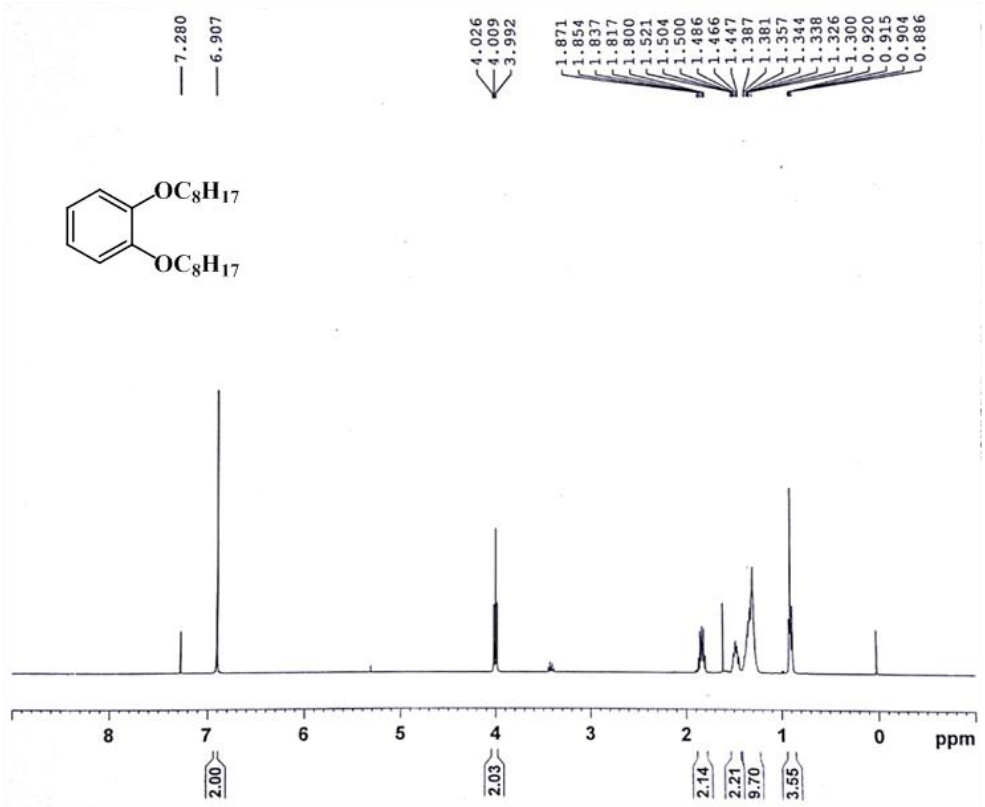

Figure 5.21 ^{1}H NMR spectrum of compound **7**

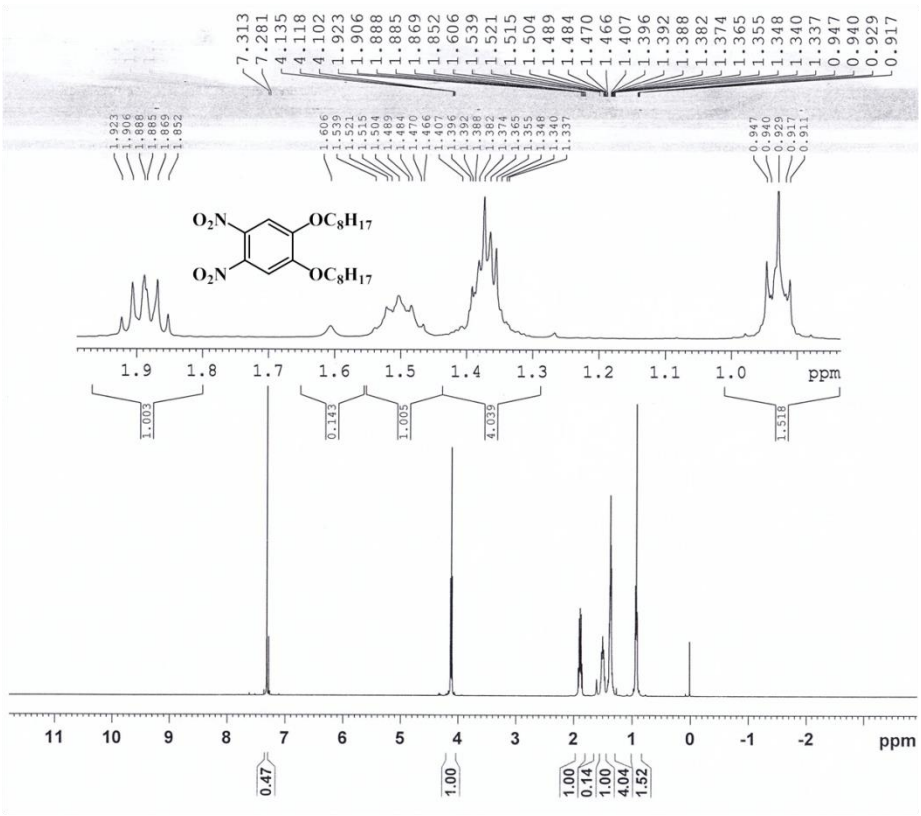

Figure 5.22 ^{1}H NMR spectrum of compound **8**

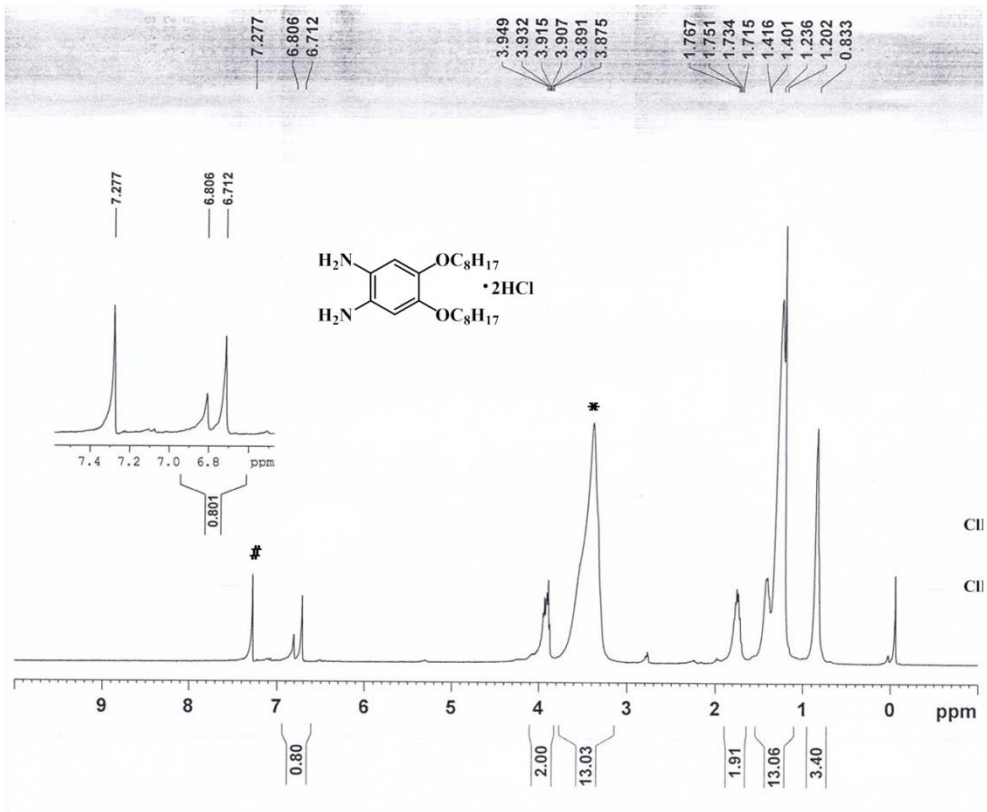

Figure 5.23 ^{1}H NMR spectrum of compound **9**; * CD_3OD and # $CDCl_3$

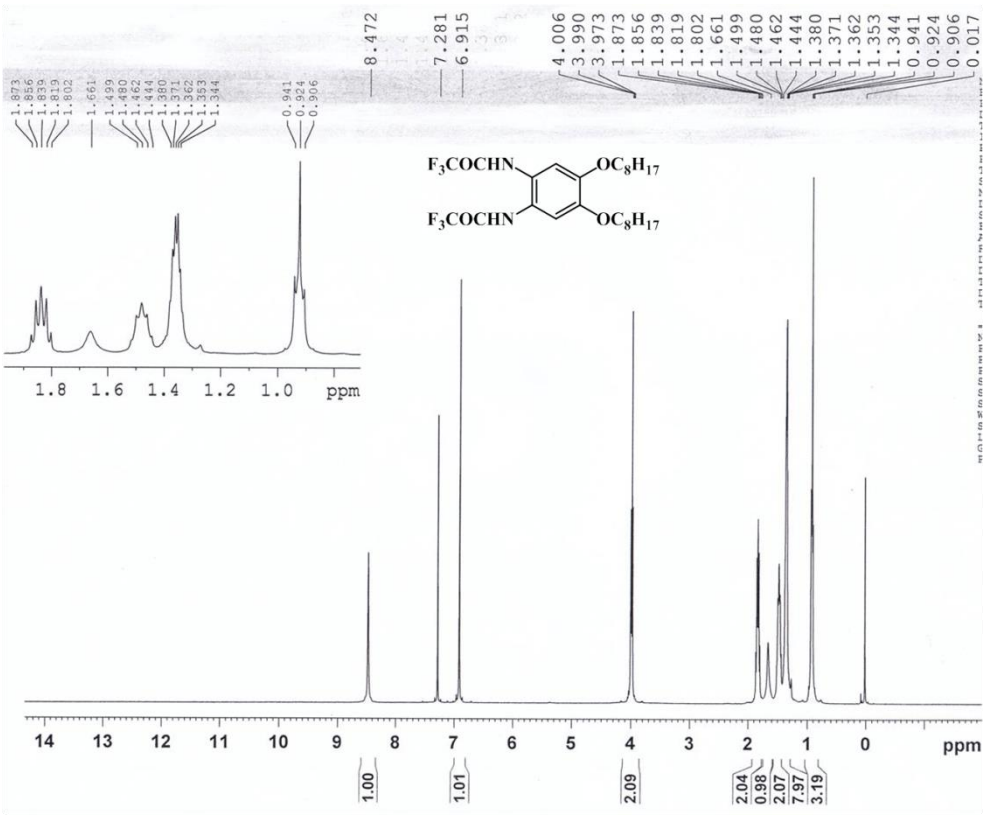

Figure 5.24 ^{1}H NMR spectrum of compound *N,N'*-(4,5-dioctyloxy-1,2 phenylene) bistrifluoroacetamide

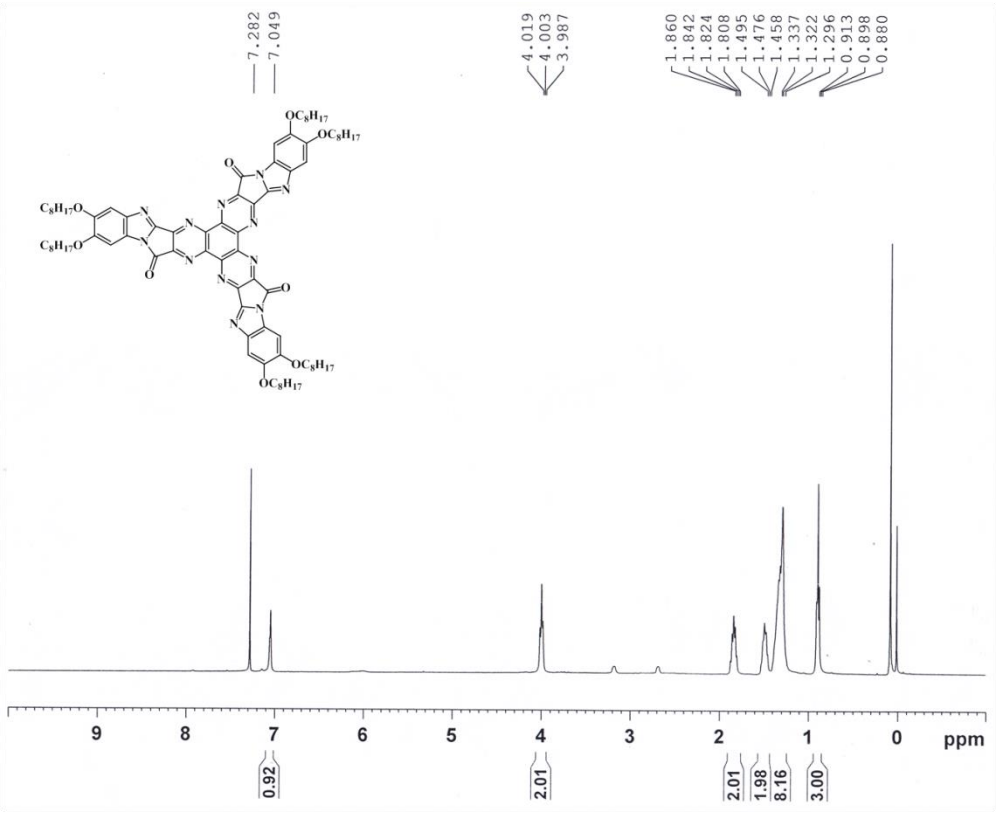

Figure 5.25 ^{1}H NMR spectrum of **HAT-IPN**

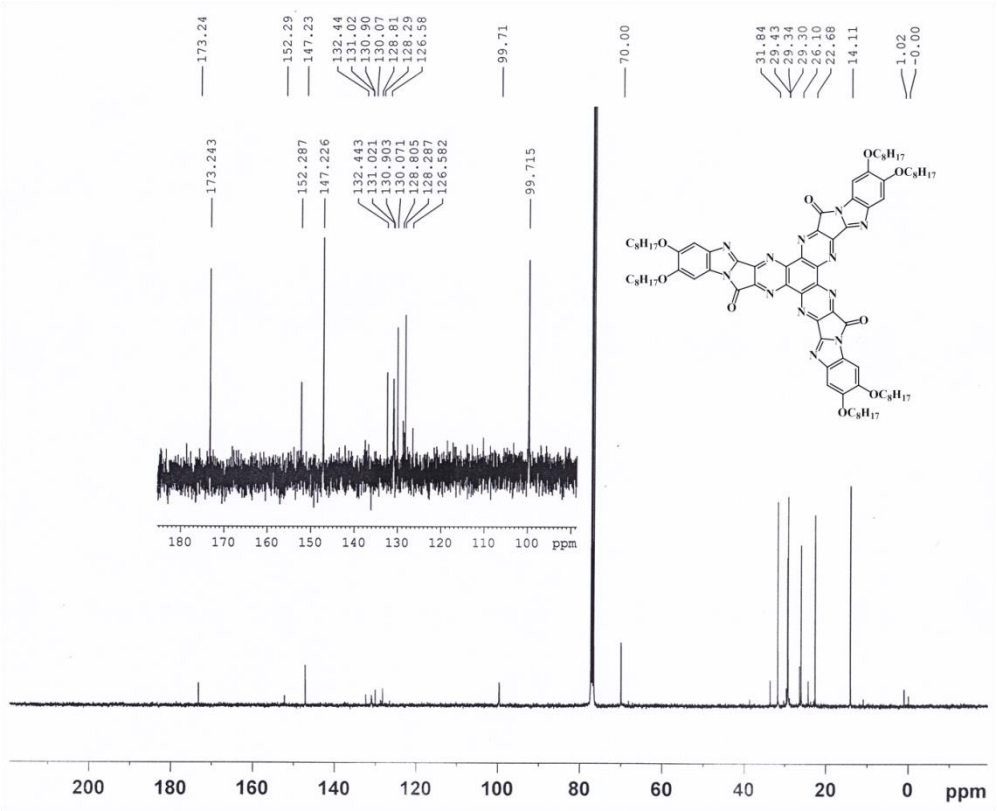

Figure 5.26 ^{13}C NMR spectrum of **HAT-IPN**

Part-B: Synthesis, photophysical, electrochemical and single crystal X-ray diffraction study of (Z)-2-phenyl-3-(5-(4-(thiophen-2-yl)benzo[*c*][1,2,5] thiadiazol-7-yl)thiophen-2-yl)acrylonitrile

Introduction

2,1,3-Benzothiadiazole (BTD) derivatives are outstanding compounds due to their electron-withdrawing properties and have been used as units of electron acceptors for conducting materials.[51–53] In the year 1970, Pilgram *et al*. synthesized BTD derivative, 4,7-dibromo-2,1,3-benzothiadiazole for the first time.[54] However, in 1996, Meijer *et al*. synthesized first BTD-based donor-acceptor (D-A) copolymer.[55] Since then, BTD unit has been frequently utilized to construct high performance D-A copolymers for organic electronics.[56,57] The BTD unit is often the electron-deficient unit of choice for molecularly hybridized push-pull type materials, where the alternating arrangement of electron rich and electron-deficient units along the π-conjugated backbone effectively controls the frontier molecular orbitals.[58,59] BTD containing compounds are expected to afford well-ordered crystal structures due to their highly polarized properties leading to intermolecular interactions such as heteroatom constants or *π*-*π* interactions.[60–63] BTD derivatives are also known as efficient fluorophores.[64] In addition to that polymers containing BTD units have been used as luminescent compounds in electroluminescence devices.[65,66] The highly electron-deficient BTD unit is one of the most popular building blocks in organic electronics. BTD can conjugatively link with an electron-rich molecule to form low band gap functional polymers or small molecules, and materials prepared in this manner showed usefulness in organic light emitting diodes (OLEDs), dye sensitized solar cells (DSSCs), light-harvesting and other optical or electronic functional devices.[67–69]

The two of the most studied push-pull type conjugated polymers in OPV research, **PCDTBT** and **PCPDTBT** are having BTD unit as electron deficient motif.[70,71] Moreover, to further fine-tune the frontier molecular orbital as well as other important materials parameters such as solubility and crystallinity, chemical modifications of the BTD unit have attracted much interest.[72–74]

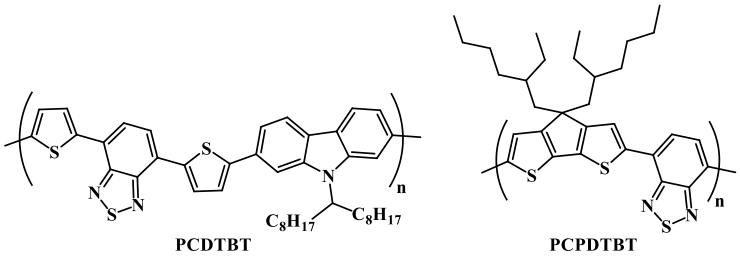

Figure 5.27 Most studied BTD-based conjugated polymers **PCDTBT** and **PCPDTBT**

The BTD unit has free 5- and 6- positions, which have proven to be useful sites to introduce either electron-donating or electron-withdrawing groups, which in turn can lead to the modified frontier molecular orbitals.[72] The dialkoxy substituted BTD derivative, **BTD-OR$_2$** is a weaker electron-withdrawing unit compared to the **BTD**, owing to the presence of electron releasing alkoxy groups attached.[73] On the other hand, 5,6-difluoro-2,1,3-benzothiadiazole (**BTD-F$_2$**) represents a stronger electron-withdrawing unit, which has led to many higher performing OPV materials. Moreover, highly electronegative fluorine atoms stabilize both lowest unoccupied molecular orbital (LUMO) and highest occupied molecular orbital (HOMO), which aid to achieve increased open-circuit voltage (V_{oc}), keeping other OPV device parameters unaffected.[75–80] Very recently, another BTD derivative, **BTD-Im** having cyclic imide ring attached to the BTD unit have been reported, which exhibited even lowered LUMO energy level due to the presence of stronger electron accepting cyclic imide. Also, the imide fused ring, attached to the BTD unit, provides a site for alkyl substitution through its nitrogen atom, which provides additional solubility advantages to the resulting polymers.[74,81,82]

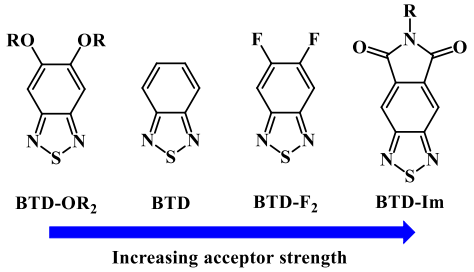

Figure 5.28 Structures of BTD-based acceptor units with varying acceptor strength

Recently, BTD-based small molecule and its selenium analogue were showed good efficiency in heterojunction solar cells and photovoltaic cells, respectively.[83–85] Alternatively, BTD- based small molecules are becoming increasingly popular for devising hybrid solar cells, because of high electron mobility and excellent chemical and physical stability of inorganic semiconductors.[86,87] Recent studies have demonstrated that formation of self-assembled monolayer of conjugated molecules on the surface of the inorganic semiconductors can lead to the formation of interfacial dipoles, which in turn, can improve the work function of substrate materials, caused by redistribution of electrons *via* charge transfer and hybridization of work functions of organic molecules and substrate surface.[88,89] These type of small conjugated molecules can act as interfacial modifiers (IMs), which enhances charge injection from metals into organic materials. J. Yu and co-workers have prepared and examined one of such IMs, having cyano-acrylic acid as anchoring group and showed increase in electron affinity at the polymer-inorganic semiconductor interface and formation of dipoles, which are oriented away from the semiconductor surface.[90] In addition, several studies involved the use of organic or Ruthenium dyes as the IMs of TiO_2 and polymers which help to increase current density (J_{sc}) of the OPV devices by enhancing light harvesting by dye molecules and cascaded electron transfer from conjugated polymer, IMs to TiO_2 as the LUMO of IMs sits between the LUMO of polymer and the conduction band of titania.[91–94]

We have synthesized BTD-based new conjugated molecule having cyano-benzylic withdrawing group, (*Z*)-2-phenyl-3-(5-(4-(thiophen-2-yl)benzo[*c*][1,2,5]thiadiazol-7-yl)thiophen-2-yl)acrylonitrile (compound **5**). The compound **5** is successfully prepared by a multi-step synthetic route. The molecular structure of compound **5** has been further confirmed by single-crystal X-ray diffraction study. The thermal and electrochemical properties of synthesized compound **5** are studied.

Results and discussion

Synthesis of compound 5

BTD-based conjugated molecule **5** is synthesized in five steps (Scheme 5.4). In the first step of the synthesis, 1,2-diaminobenzene was treated with thionyl chloride ($SOCl_2$) to achieve 2,1,3-benzthiadiazole **1** in 36% yield, which on further treated with

Br_2 in HBr (48 % aqueous) to get 4,7-dibromo-2,1,3-benzothiadizole, **2** in 68% yield. Compound **2** was further treated with 2-(tri-*n*-butylstannyl)thiophene in presence of $Pd(PPh_3)_2Cl_2$ to get compound **3** in 49% yield. Monoformylation of compound **3** using the Vilsmeier-Haack reaction conditions gives compound **4** in 56% yield, which was subjected to Knoevenagel condensation reaction with benzyl cyanide to get desired compound **5** in 62 % yield.

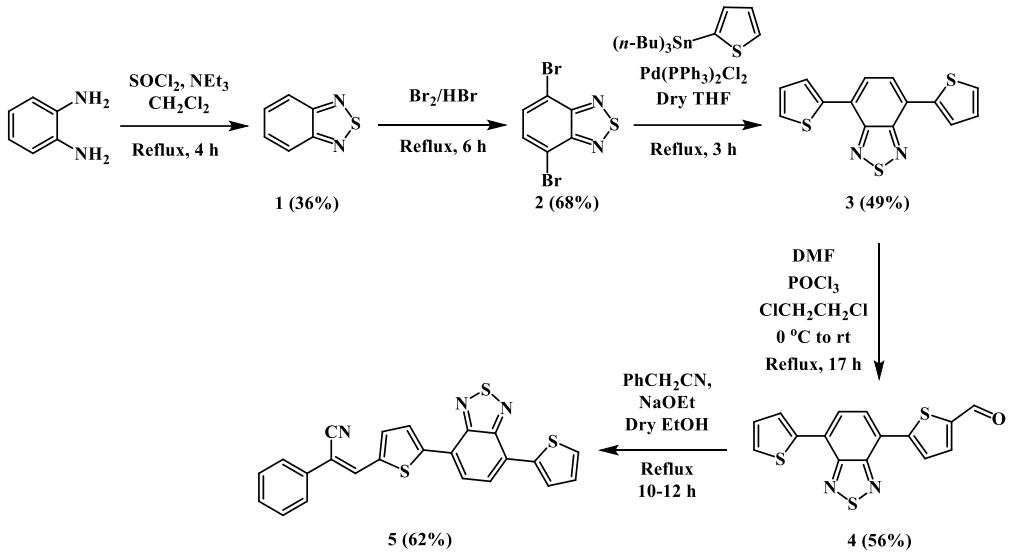

Scheme 5.4 Synthesis of (*Z*)-2-phenyl-3-(5-(4-(thiophen-2-yl)benzo[*c*][1,2,5]thiadiazol-7-yl)thiophen-2-yl)acrylonitrile (compound **5**)[95]

Single crystal X-ray diffraction (SCXRD) study of compound 5

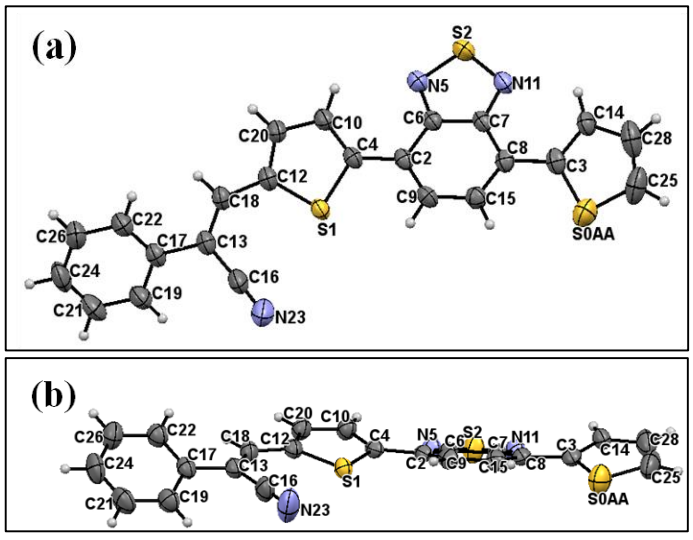

Figure 5.29 ORTEP drawing of crystal structure of compound **5**; (a) top view and (b) side view

X-ray structure of compound **5** clearly suggest that it crystallizes in monoclinic system with space group $P2_1/c$. Asymmetric unit of this contains a full molecule and

there are four such molecules present in the unit cell. The unit cell parameters are: a = 16.9905 (7); b = 7.2712 (3), c = 16.5005 (7) and α = 90.00, β = 107.130 (4) and ϒ = 90.00.

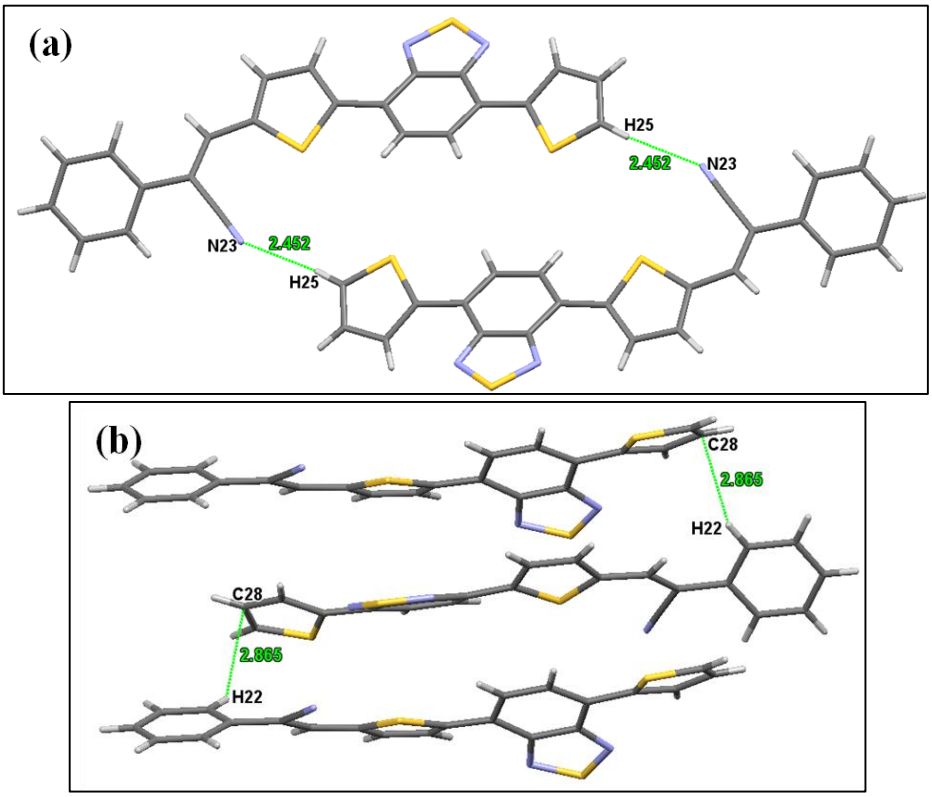

Figure 5.30 Arrangement of neighbouring molecules in the crystal packing of compound **5** *via* (a) C−H···N interaction along *b* axis and (b) C−H···π interaction along *c* axis

Notably, the presence of various polar sub-units in the molecular framework of compound **5** induces conformational changes in the molecule, which apparently changes the nature and number of donor-acceptors sites. For instance, all the heterocyclic as well carbocyclic rings present in compound **5** are not co-planar, making differential dihedral angles with one-another *ca.* a dihedral angle between the least squares planes drawn through peripheral thiophene ring and adjacent benzothiadiazole ring is estimated 24.24°, whereas a dihedral angle between the least squares planes drawn through internal thiophene ring and adjacent benzothiadiazole ring is estimated 23.18° and *vice versa*. In fact, the crystal structure of compound **5** is sustained by a number of weak non-bonding intermolecular forces of attraction such as C−H···N, C−H···π donor-acceptor interactions as shown in the following Figure 5.30a and b. Interestingly, C−H···N (H25···N23) donor-acceptor interaction limits the growth of molecular packing along the *a*-axis by forming a closed contact (Figure 5.30a).

However, C−H···π (H22···C28) donor-acceptor interactions arranged the molecules of **5** along the *b*-axis and forming a *zig-zag* networking as shown in Figure 5.30b. Moreover, compound **5** exhibits various molecular packing patterns along the *a*, *b* and *c* axis as shown in Figure 5.31 a, b and c.

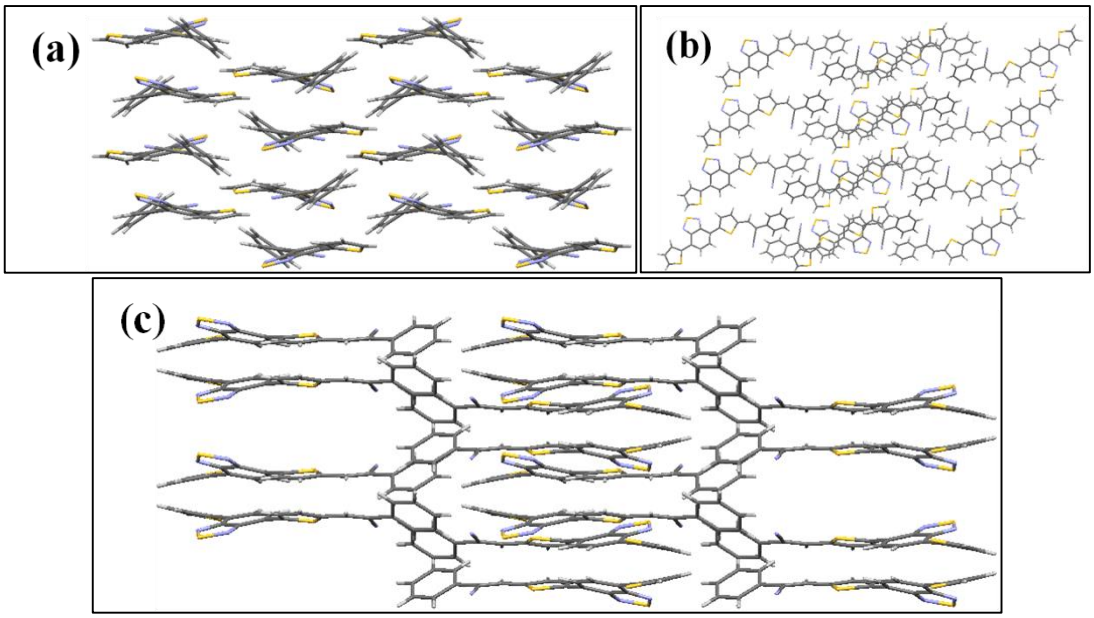

Figure 5.31 Various molecular packing patterns of compound **5**; (a) along *a*-axis; (b) along *b*-axis and (c) along *c*-axis

Table 5.1 Crystallographic data and structures refinement parameters

Parameters	Values	Parameters	Values
Identification code	Compound **5**	Volume/Å^3	1948.07(14)
Empirical formula	$C_{23}H_{15}N_3S_3$	Z	4
Formula weight	429.56	ρ_{calc}g/cm^3	1.465
Temperature/K	293 (2)	Crystal size/mm^3	0.09×0.07×0.05
Crystal system	Monoclinic	Radiation	Mo Kα (λ = 0.71073)
Space group	$P2_1/c$	Reflections collected	11899
a/Å	16.9905(7)	Independent reflections	4596[R_{int} = 0.0363]
b/Å	7.2712(3)	Data/restraints/parameters	4596/0/262
c/Å	16.5005(7)	Goodness-of-fit on F^2	1.042
α/°	90.00	Final R indexes [I>=2σ (I)]	R1 = 0.0539, wR2 = 0.1423
β/°	107.130(4)	Final R indexes [all data]	R1 = 0.0729, wR2 = 0.1565
γ/°	90.00	Largest diff. peak/hole/eÅ^{-3}	0.48/-0.57
		CCDC Number	**1431814**

Photo-physical properties of compound 5

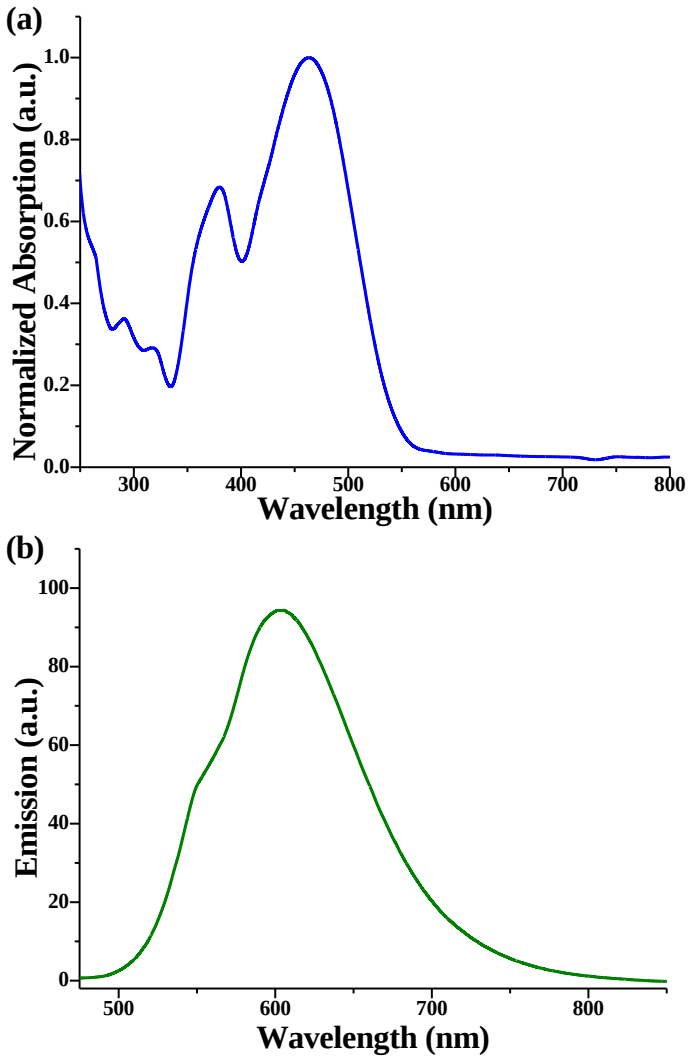

Figure 5.32 (a) Absorption spectra and (b) Emission spectra of compound **5**, measured in methanol solution

The photo-physical property of compound **5** was studied using UV-visible spectroscopy and fluorescence spectroscopy. The absorption and emission spectra of **5** were carried out in methanol (Figure 5.32a). Compound **5** exhibited the multiple band absorption spectrum with complex splitting pattern in the solution state. One lower energy band is ranging in between 250-334 nm which is due to π-π^* transition of the conjugated backbones, while the second and third higher energy bands are ranging between 335-400 nm (λ_{max} 379 nm) and 401-520 nm (λ_{max} 463 nm), respectively which can be ascribed to the charge transfer transition between donor and acceptors. The steady state fluorescence spectrum of compound **5** in methanol (Figure 5.32b) showed emission at 603 nm, with stokes shift of 140 nm when excited at 463 nm by a single monochromatic beam.

Electrochemical properties of compound 5

The frontier orbital energy levels of the synthesized compound **5** were measured using cyclic voltammetry (CV). CV experiments were performed in the dry THF using $TBAPF_6$ as a supporting electrolyte (~50 mM) with a three electrode system: a glassy carbon electrode as the working electrode, a Pt wire electrode as the counter electrode and non-aqueous Ag/Ag^+ as the reference electrode. Ferrocene/ferrocenium redox couple was used as an internal standard. As shown in Figure 5.33, compound **5** exhibits an irreversible oxidation with an anodic peak potential of +1.92 V. The highest occupied molecular orbital (HOMO) energy level was then calculated from the oxidation potential (E_{oxi}), according to the formula $E_{HOMO} = -[(E_{oxi} - E_{(Fc/Fc+)}) + 4.8\ eV]$, where $E_{(Fc/Fc+)}$ denotes the measured oxidation potential of ferrocene and 4.8 eV is the absolute oxidation potential value of ferrocence under vacuum. Calculated value of E_{HOMO} for compound **5** is –5.86 eV and value of E_{LUMO} is –3.59 eV which is calculated from the formula $E_{LUMO} = [E_{HOMO} + E_g^{Opt}]$.

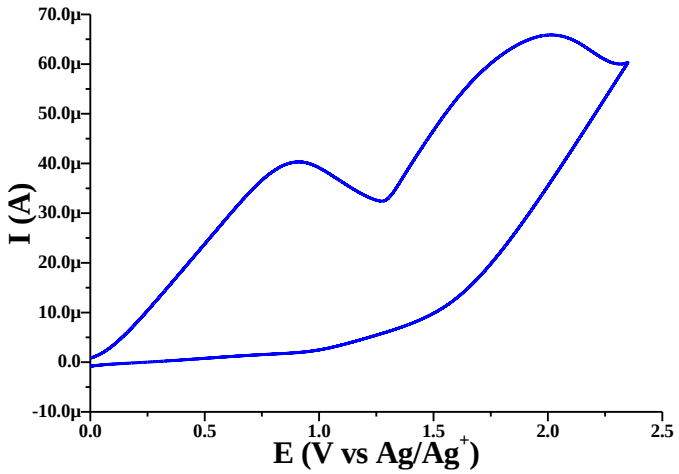

Figure 5.33 Cyclic voltammogram of compound **5** in dry THF, using $TBAPF_6$ as supporting electrolyte and ferrovene as internal standard, scanned at 100 mV/s; $E_{(Fc/Fc+)}$ = +0.86 V

Thermogravimetric analysis of compound 5

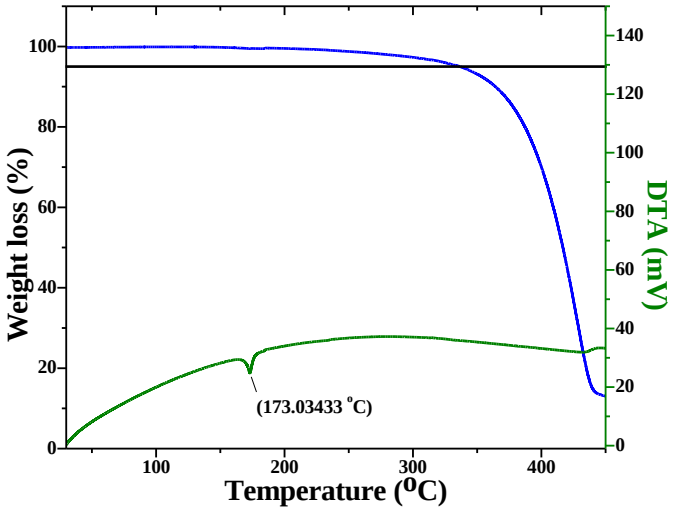

Figure 5.34 Thermogravimetric analysis of compound **5**; TG curve (blue solid line) and DTA curve (green solid line)

Thermal properties of the synthesized BTD-based compound **5** were analyzed by thermogravimetric analysis (TGA) at a heating rate of 10 °C/min under nitrogen atmosphere (Figure 5.34; blue solid line). Compound **5** showed reasonably good thermal stability up to 330 °C with a decomposition temperature, T_d of 336 °C. As the DTA curve shows, phase transition was observed at 173.03 °C for compound **5** (Figure 5.34; green solid line), which is also in accordance with melting point of compound **5** (173-175 °C).

Conclusion

The BTD-based small conjugated molecule, having alternating donor and acceptor units, (*Z*)-2-phenyl-3-(5-(4-(thiophen-2-yl)benzo[*c*][1,2,5]thiadiazol-7-yl)thiophen-2-yl)acrylonitrile (compound **5**) was synthesized by mono-formylation of 4,7-di(thiophen-2-yl)-2,1,3-benzothiadiazole followed by Knoevenagel condensation reaction with benzyl cyanide. The synthesized compound **5** is well characterized by ^{1}H and ^{13}C NMR spectroscopy, Mass spectroscopy, IR spectroscopy and single crystal X-ray diffraction (SCXRD) spectroscopy. This novel compound was screened for its band-gap properties using UV-visible spectroscopy, cyclic-voltametry and theoretical calculations using density functional theory. Thermal stability of the synthesized molecule is studied using thermogravimetric analysis. The experimental data shows

that compound **5** could be a potential candidate as an interfacial modifier for photovoltaic devices.

Experimental procedures

General procedures

All the chemicals were reagent grade and used as purchased. Moisture-sensitive reactions were performed under an inert atmosphere of dry nitrogen with dried solvents. Reactions were monitored by TLC analysis using Merck 60 F_{254} aluminium coated plates and the spots were visualized under UV light. Column chromatography was carried out on Silica gel (60-120 mesh). All melting points were determined using Thiele's tube using paraffin oil and are uncorrected. IR spectra were recorded on a Shimadzu Prestige 21 spectrometer. Mass spectra were recorded on Thermo-Fischer DSQ II GCMS instrument. NMR spectra were recorded on a Bruker Avance-III 400 MHz spectrometer in $CDCl_3$. Diffraction data were collected using Mo Kα (λ = 0.71073) radiation on an Xcalibur, Eos, Gemini diffractometer. CV data were obtained with CH Instruments model of CHI 600C with three electrode (glassy carbon as the working electrode, platinum as the counter electrode, and non-aqueous $Ag/AgNO_3$ as the reference electrode) cells in anhydrous THF solution containing 0.1 M tetra-*n*-butylammonium hexafluorophosphate ($TBAPF_6$) at a scan rate of 100 mV s^{-1} under N_2 atmosphere. DFT calculations were performed using Gaussian 09 program with B3LYP functional and 6-311G (++) basis set.[46]

Synthesis of compounds **1** and **2**: Compounds **1** and **2** were synthesized according to the literature procedures reported by Neto *et al*.[96] and Yu *et al*.[90] The detailed synthetic procedures are given in Chapter 2.

Compound **1**[96]: White solid; ^{1}H NMR (400 MHz, $CDCl_3$): 8.00−8.05 (dd, J_1 = 6.8 Hz, J_2 = 3.2 Hz, 1H), 7.59−7.63 (dd, J_1 = 6.8 Hz, J_2 = 3.2 Hz, 1H). ESI-Mass 135.90 [M+] (100.0%), 135.17 [M−1(-H)] (42.4%).

Compound **2**[90]: Off-white solid; ^{1}H NMR (400 MHz, $CDCl_3$): 7.75 (s, 1H). ESI-Mass 293.39 [M+] (100.0%), 291.39 [M−2] (50.2%).

Synthesis of 4,7-di(thiophen-2-yl)-2,1,3-benzothiadiazole (compound **3**): Compound **2** (1.00 g, 3.4 mmol) was taken in a dry two necked round bottom flask and

is dissolved in dry THF (25 mL). To this stirred solution, $Pd(PPh_3)_2Cl_2$ (0.12 g, 0.17 mmol) and 2-(tri-*n*-butylstannyl)thiophene (2.37 mL, 7.48 mmol) were added under nitrogen atmosphere and resulting reaction mixture was refluxed for 10-12 h under nitrogen atmosphere. After cooling, the reaction mixture was quenched with water and extracted with ethyl acetate (2 X 50 mL). Combined organic layers were washed with water, brine, dried over anhydrous sodium sulfate and evaporated to dryness under reduced pressure. The crude product was purified using column chromatography over silica gel and the pure product was eluted using 10% ethyl acetate-petroleum ether mobile phase. The pure product was further recrystallized in petroleum ether.

4,7-di(thiophen-2-yl)-2,1,3-benzothiadiazole (compound **3**): Orange yellow solid (0.50 g, 49%); Melting point: 123-124 ^oC. ^1H NMR (400 MHz, $CDCl_3$): 8.13−8.14 (dd, J_1 = 3.6 Hz, J_2 = 1.2 Hz, 1H), 7.88 (s, 2H), 7.47−7.48 (dd, J_1 = 5.2, J_2 = 1.2 Hz, 2H), 7.22−7.24 (m, 2H). ^{13}C NMR (100 MHz, $CDCl_3$): 152.6, 139.4, 128.0, 127.5, 126.8, 126.0, 125.8. ESI-Mass (m/z): 300.06 [M+] (100 %), 299.12 (90 %), 80.89 (15 %), 68.64 (22 %). IR (KBr, cm^{-1}): 2978, 2885, 2389, 1725, 1562, 1481, 1013, 823, 772, 692.

Synthesis of 5-(4-(thiophen-2-yl)benzo[*c*][1,2,5]thiadiazol-7-yl)thiophene-2-carbaldehyde (compound **4**): In a two necked round bottom flask, DMF (0.39 mL, 5 mmol) was taken, cooled to 0 ^oC and kept under nitrogen atmosphere for 15 min. To this stirred solution, $POCl_3$ (0.47 mL, 5 mmol) was added drop wise and stirred for 15 min at the same temperature. The solution of compound **3** (0.150 g, 0.5 mmol in 20 mL of dichloroethane) was added drop wise to this and the resulting reaction mixture was refluxed for 17 h. After cooling the reaction mixture, saturated aqueous sodium acetate solution (50 mL) was added to the reaction mixture and stirred for 2 h at room temperature. The crude compound was extracted with aliquots of dichloromethane (2 X 25 mL) and the combined organic layer was washed with water, brine, dried over anhydrous sodium sulfate and evaporated to dryness under vacuum. The resulting crude product was purified by column chromatography over silica gel and pure product was eluted using 20% ethyl acetate-petroleum ether as eluent.

5-(4-(thiophen-2-yl)benzo[c][1,2,5]thiadiazol-7-yl)thiophene-2-carbaldehyde (compound **4**): Reddish orange solid (0.092 g, 56%); Melting point: 168-170 ^oC. ^1H NMR (400 MHz, $CDCl_3$): 10.00 (s, 1H), 8.23−8.24 (d, J = 4.0 Hz, 1H), 8.20−8.21 (dd,

J_1 = 4.0 Hz, J_2 = 1.2 Hz, 1H), 8.02−8.04 (d, J = 7.6 Hz, 1H), 7.94−7.96 (d, J = 7.6 Hz, 1H), 7.86−7.88 (d, J = 4.4 Hz, 1H), 7.53−7.54 (dd, J_1 = 4.8 Hz, J_2 = 1.2 Hz, 1H), 7.25−7.27 (m, 1H). ^{13}C NMR (100 MHz, $CDCl_3$): 183.1, 152.5, 152.4, 148.6, 143.4, 138.9, 136.9, 128.4, 128.2, 128.1, 127.9, 127.8, 127.4, 125.3, 124.3. IR (KBr, cm^{-1}): 2983, 2888, 2410, 1655, 1440, 1236, 834, 818.

Synthesis of (Z)-2-phenyl-3-(5-(4-(thiophen-2-yl)benzo[*c*][1,2,5]thiadiazol-7-yl)thiophen-2-yl)acrylonitrile (compound **5**): A mixture of compound **4** (0.1 g, 0.305 mmol) and benzyl cyanide (0.038 g, 0.32 mmol) was taken in a single neck round bottom flask and was dissolved in 30 mL of dry ethanol. In a separate single neck round bottom flask, small pieces of sodium metal (0.031 g, 1.53 mmol) were slowly dissolved into the 10 mL of dry ethanol and the resulting solution was added drop wise to the reaction mixture at room temperature. The resulting reaction mixture was refluxed for 10-12 h. After completion of the reaction, excess of ethanol is distilled out. The crude product is purified by column chromatography over silica gel and the pure product was eluted using 20% ethyl acetate-petroleum ether as eluent.

(Z)-2-phenyl-3-(5-(4-(thiophen-2-yl)benzo[c][1,2,5]thiadiazol-7-yl)thiophen-2-yl)acrylonitrile (compound **5**): Dark red solid (0.08 g, 62%); Melting point: 173-175 ^{o}C. ^{1}H NMR (400 MHz, $CDCl_3$): 8.21−8.22 (dd, J_1 = 4.0 Hz, J_2 = 0.8 Hz, 1H), 8.16−8.17 (dd, J_1 = 4.0 Hz, J_2 = 1.2 Hz, 1H), 7.97−7.99 (dd, J_1 = 7.2 Hz, J_2 = 1.2 Hz, 1H), 7.89−7.91 (dd, J_1 = 7.6 Hz, J_2 = 0.8 Hz, 1H), 7.73−7.74 (d, J = 4.0 Hz, 1H), 7.68−7.70 (m, 3H), 7.49−7.51 (m, 1H), 7.45−7.47 (d, J = 8.0 Hz, 2H), 7.38−7.42 (m, 1H), 7.23−7.25 (m, 1H). ^{13}C NMR (100 MHz, $CDCl_3$): 152.6, 152.5, 143.7, 139.1, 138.5, 133.9, 133.8, 133.7, 129.1, 129.0, 128.1, 128.0, 127.4, 127.1, 126.6, 125.7, 125.5, 124.8, 118.3, 108.2. IR (KBr, cm^{-1}): 2983, 2897, 2390, 2289, 1583, 1480, 1439, 828, 801, 756, 720, 690.

Spectral data

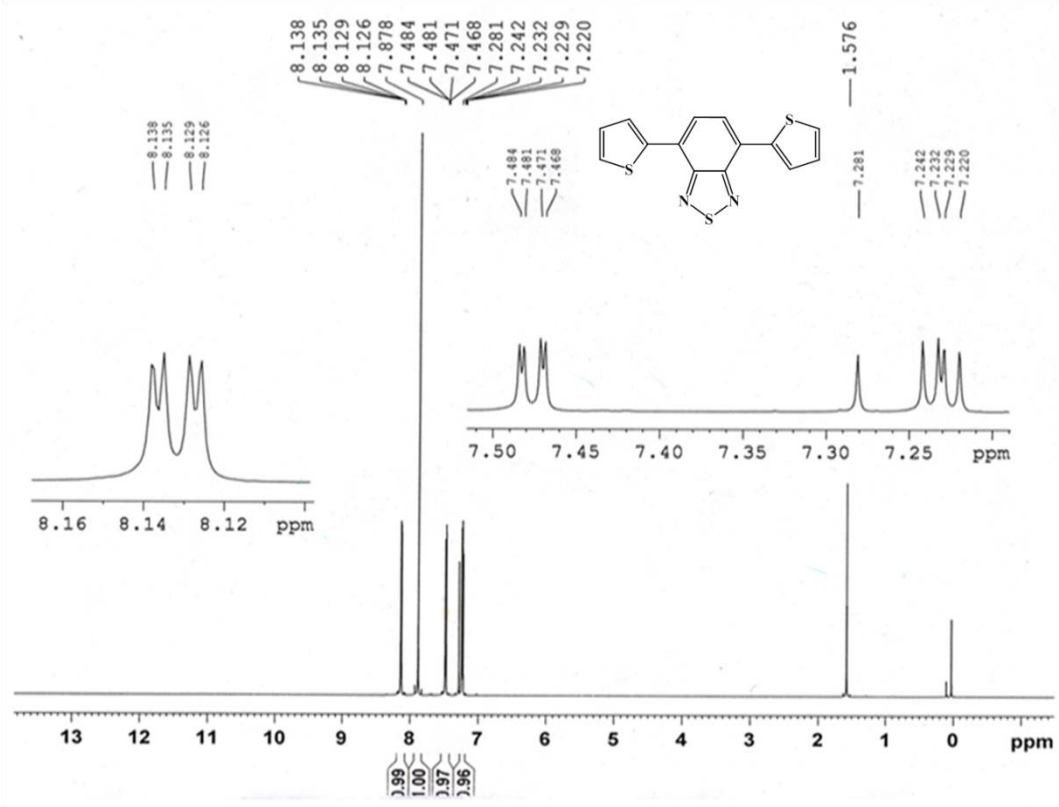

Figure 5.35 ^{1}H NMR spectrum of compound **3**

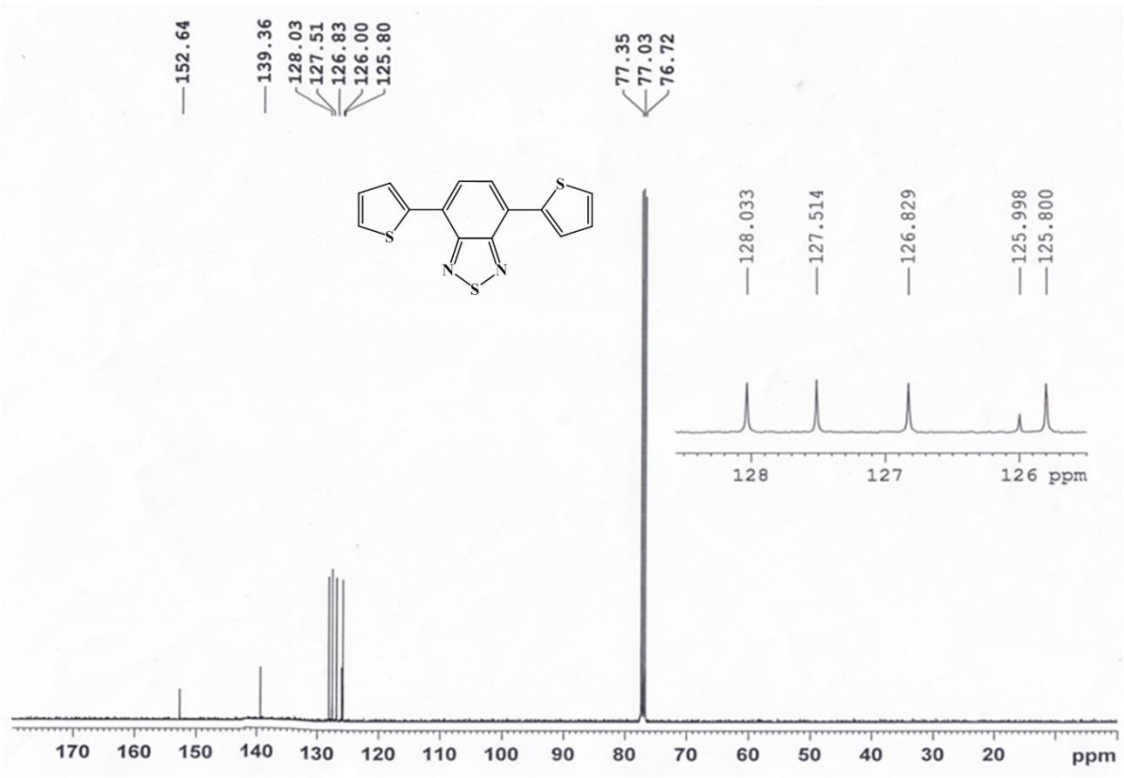

Figure 5.36 ^{13}C NMR spectrum of compound **3**

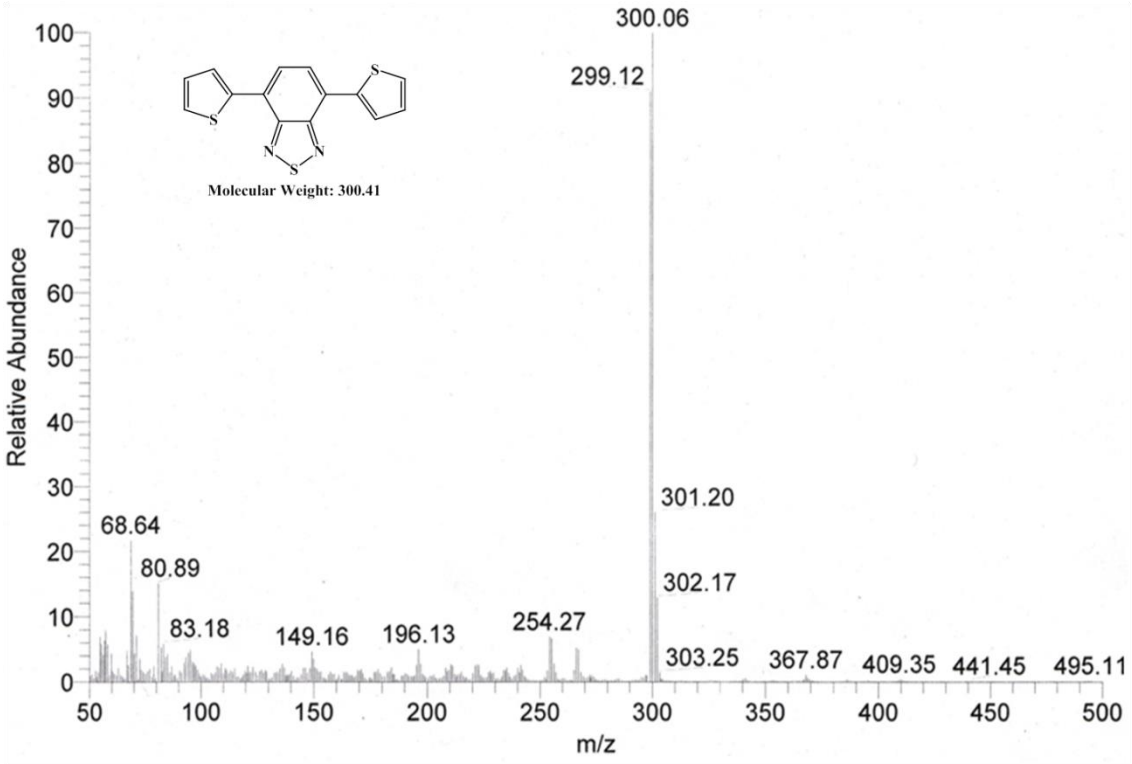

Figure 5.37 ESI-Mass spectrum of compound **3**

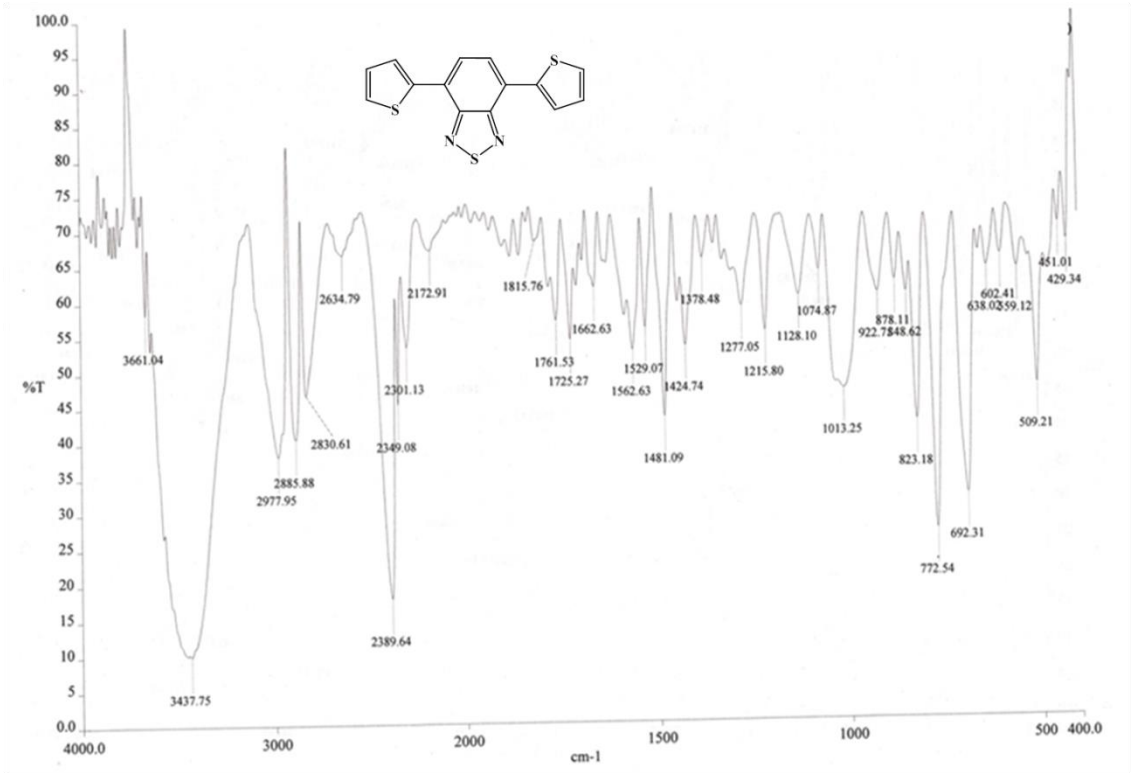

Figure 5.38 IR spectrum (KBr pellet) of compound **3**

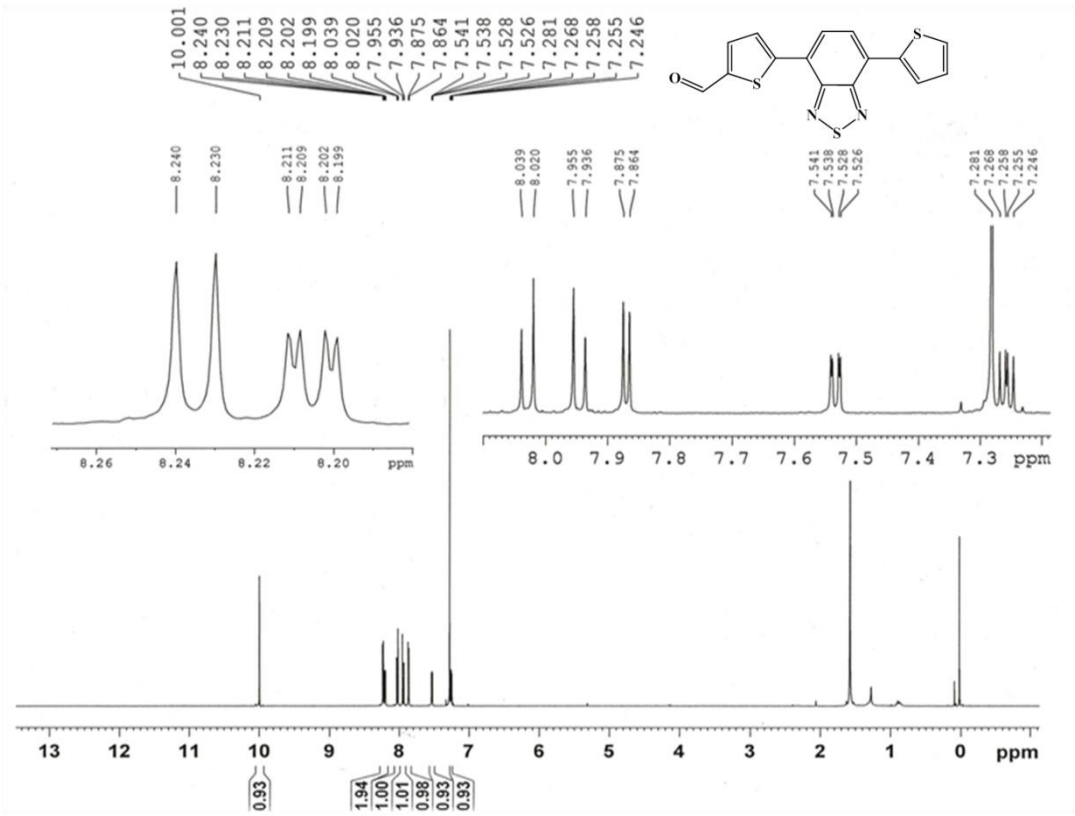

Figure 5.39 ^{1}H NMR spectrum of compound **4**

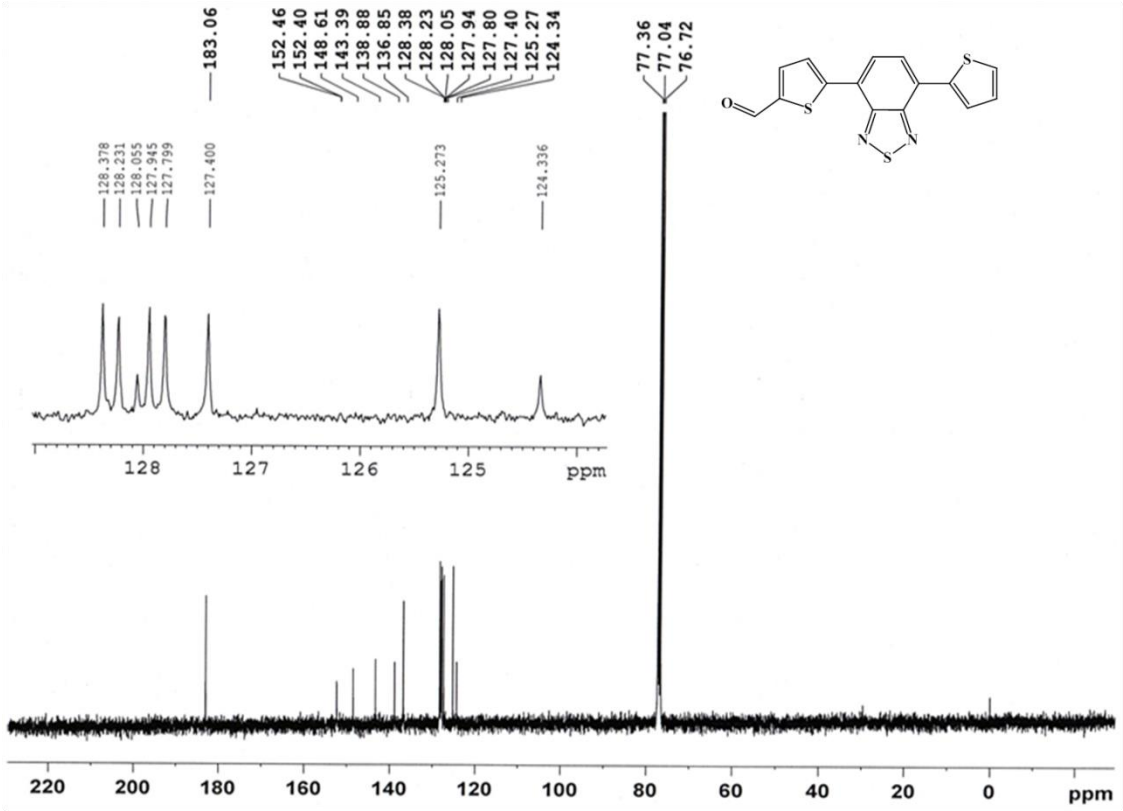

Figure 5.40 ^{13}C NMR spectrum of compound **4**

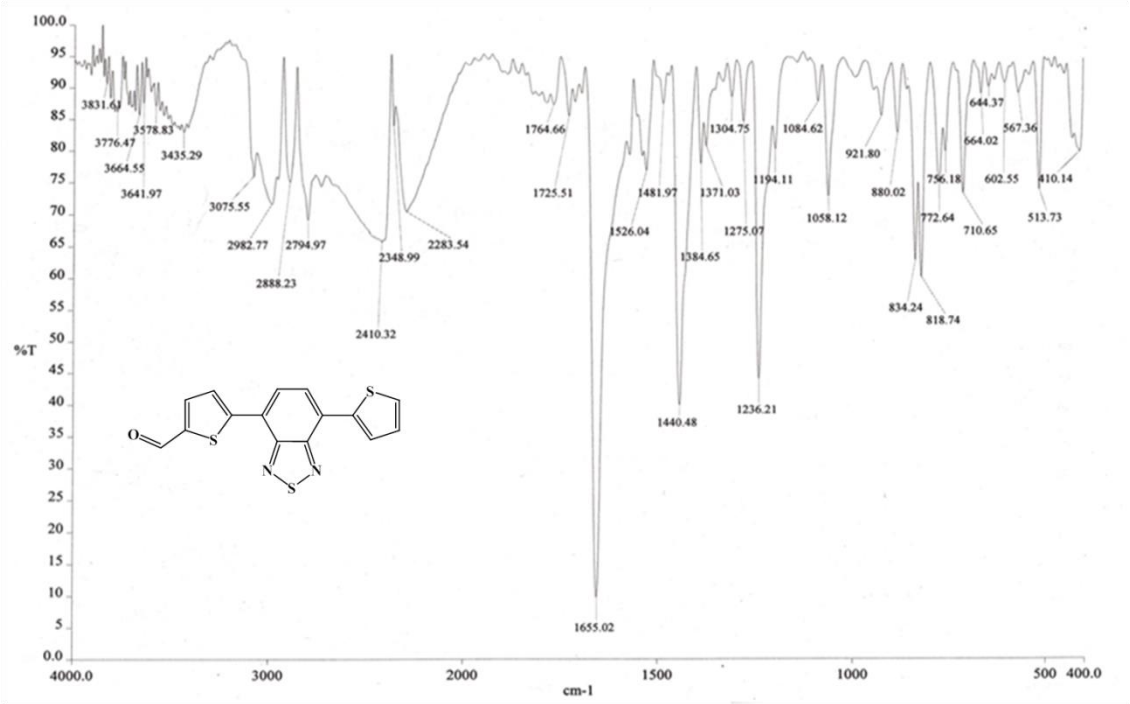

Figure 5.41 IR spectrum (KBr pellet) of compound **4**

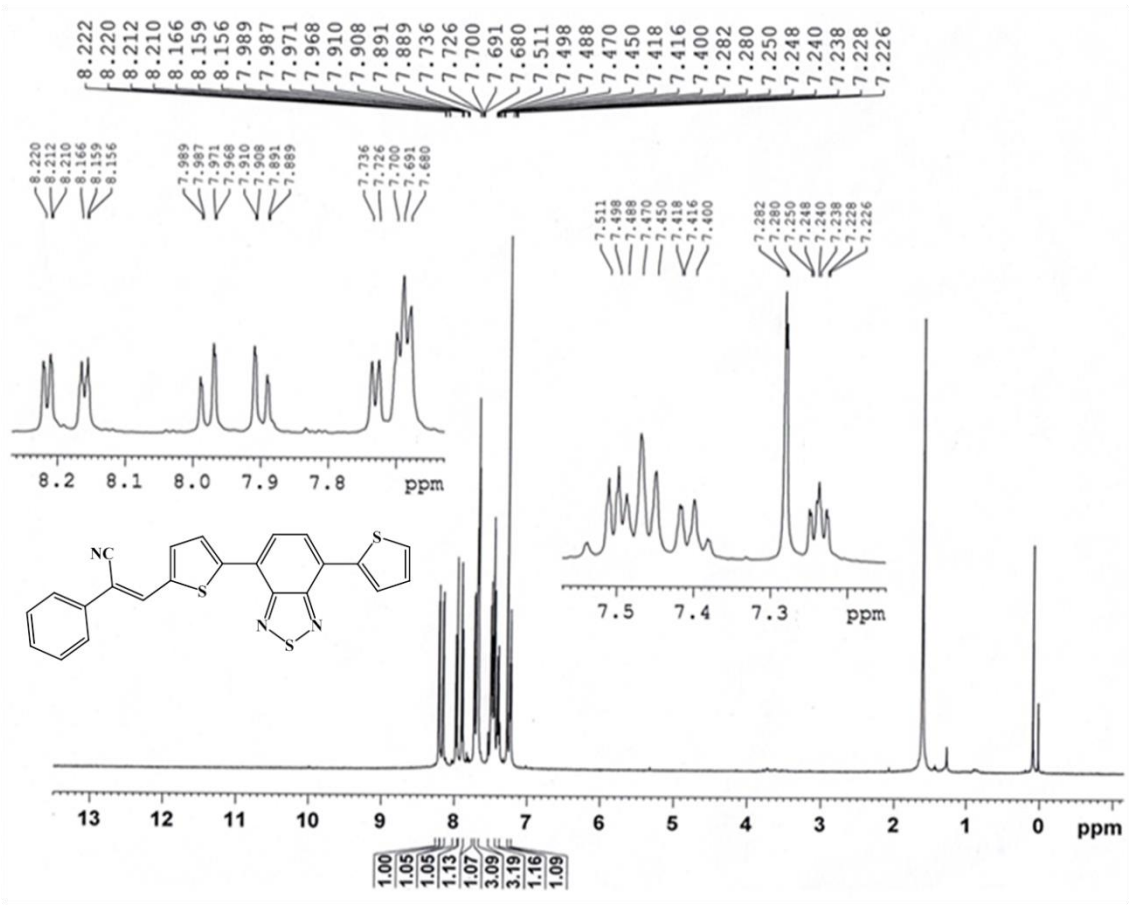

Figure 5.42 ^{1}H NMR spectrum of compound **5**

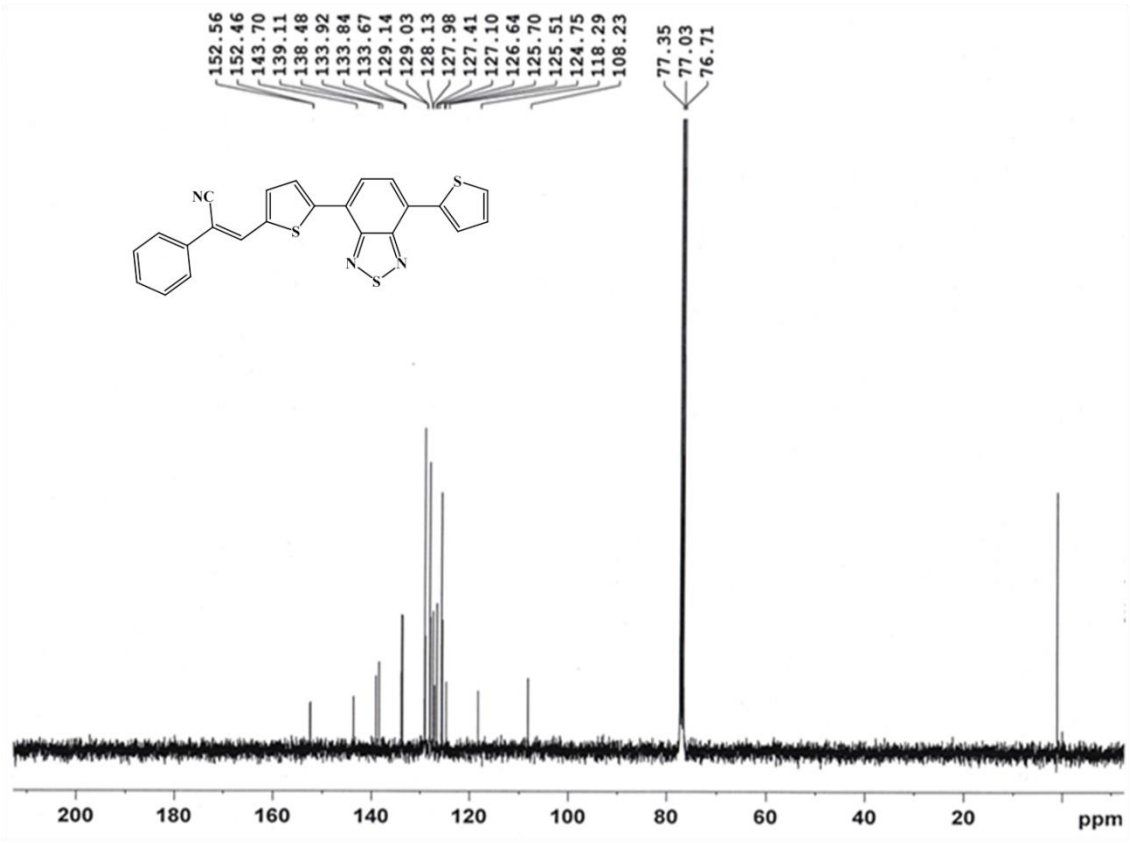

Figure 5.43 ^{13}C NMR spectrum of compound **5**

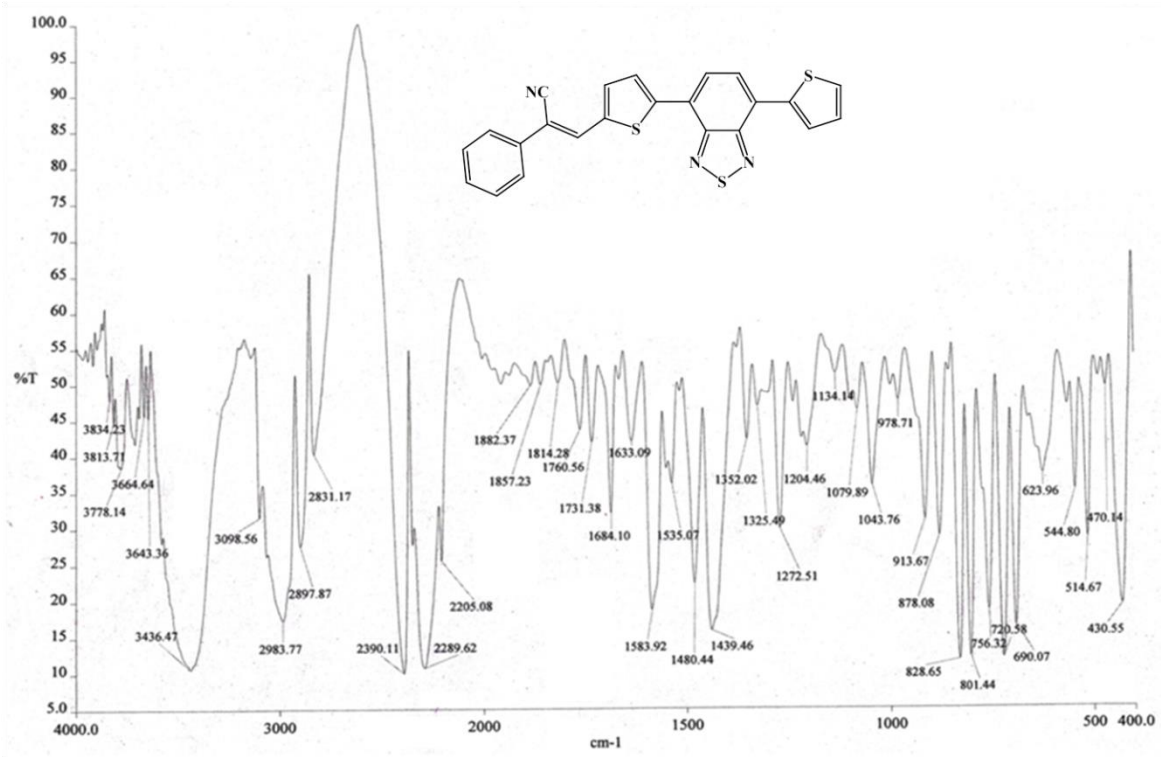

Figure 5.44 IR spectrum (KBr pellet) of compound **5**

References

1 J. Wu, W. Pisula and K. Müllen, *Chem. Rev.*, 2007, **107**, 718–747.

2 M. Bendikov, F. Wudl and D. F. Perepichka, *Chem. Rev.*, 2004, **104**, 4891–4946.

3 S. S. Zade and M. Bendikov, *Angew. Chemie Int. Ed.*, 2010, **49**, 4012–4015.

4 J. E. Anthony, *Chem. Rev.*, 2006, **106**, 5028–5048.

5 D. Biermann and W. Schmidt, *J. Am. Chem. Soc.*, 1980, **102**, 3163–3173.

6 U. H. F. Bunz, J. U. Engelhart, B. D. Lindner and M. Schaffroth, *Angew. Chem. Int. Ed. Engl.*, 2013, **52**, 3810–3821.

7 L. Chen, Y. Hernandez, X. Feng and K. Müllen, *Angew. Chemie Int. Ed.*, 2012, **51**, 7640–7654.

8 J. Zaumseil and H. Sirringhaus, *Chem. Rev.*, 2007, **107**, 1296–1323.

9 J. L. Segura, R. Juárez, M. Ramos and C. Seoane, *Chem. Soc. Rev.*, 2015, **44**, 6850–6885.

10 J. M. Mativetsky, M. Kastler, R. C. Savage, D. Gentilini, M. Palma, W. Pisula, K. Müllen and P. Samorì, *Adv. Funct. Mater.*, 2009, **19**, 2486–2494.

11 Z. U. Levi and T. D. Tilley, *J. Am. Chem. Soc.*, 2010, **132**, 11012–11014.

12 R. I. Gearba, M. Lehmann, J. Levin, D. A. Ivanov, M. H. J. Koch, J. Barberá, M. G. Debije, J. Piris and Y. H. Geerts, *Adv. Mater.*, 2003, **15**, 1614–1618.

13 Z. Xu, M. Wang, J. Zhao, C. Cui, W. Fan and J. Liu, *Electrochim. Acta*, 2014, **125**, 241–249.

14 M. L. Tang, A. D. Reichardt, P. Wei and Z. Bao, *J. Am. Chem. Soc.*, 2009, **131**, 5264–5273.

15 K. C. Moss, K. N. Bourdakos, V. Bhalla, K. T. Kamtekar, M. R. Bryce, M. A. Fox, H. L. Vaughan, F. B. Dias and A. P. Monkman, *J. Org. Chem.*, 2010, **75**, 6771–6781.

16 V. M. Blas-Ferrando, J. Ortiz, J. Follana-berna, F. Fernández-Lázaro, A. Campos, M. Mas-Torrent and A. Sastre-Santos, *Org. Lett.*, 2016, **18**, 1466–1469.

17 S. Chandrasekhar, in *Handbook of Liquid Crystals*, eds. D. Demus, J. W. Goodby, G. W. Gray, H.-W. Spiess and V. Vill, Wiley-VCH Verlag GmbH, Weinheim, Germany, Second Edi., 1998, p. 749.

18 D. Guillon, in *Structure and Bonding: Liquid Crystals II*, ed. D. M. P. Mingos, Springer, Verlag, Berlin, Germany, 1999, pp. 41–82.

19 T. Ishi-i, K. Yaguma, R. Kuwahara, Y. Taguri and S. Mataka, *Org. Lett.*, 2006, **8**, 585–588.

20 L. Huang, C. Liu, X. Qiao, H. Tian, Y. Geng and D. Yan, *Adv. Mater.*, 2011, **23**,

3455–3459.

21 J. E. Norton and J.-L. Brédas, *J. Chem. Phys.*, 2008, **128**, 34701.

22 Y. Zhang, H. Dong, Q. Tang, S. Ferdous, F. Liu, S. C. B. Mannsfeld, W. Hu and A. L. Briseno, *J. Am. Chem. Soc.*, 2010, **132**, 11580–11584.

23 P. Strohriegl and J. V. Grazulevicius, *Adv. Mater.*, 2002, **14**, 1439–1452.

24 T. Aoki, H. Sakai, K. Ohkubo, T. Sakanoue, T. Takenobu, S. Fukuzumi and T. Hasobe, *Chem. Sci.*, 2015, **6**, 1498–1509.

25 L. M. Klivansky, D. Hanifi, G. Koshkakaryan, D. R. Holycross, E. K. Gorski, Q. Wu, M. Chai and Y. Liu, *Chem. Sci.*, 2012, **3**, 2009–2014.

26 T. Ishi-i, K. Murakami, Y. Imai and S. Mataka, *Org. Lett.*, 2005, **7**, 3175–3178.

27 M. Wang, Y. Li, H. Tong, Y. Cheng, L. Wang, X. Jing and F. Wang, *Org. Lett.*, 2011, **13**, 4378–4381.

28 S. Choudhary, C. Gozalvez, A. Higelin, I. Krossing, M. Melle-Franco and A. Mateo-Alonso, *Chem. - A Eur. J.*, 2014, **20**, 1525–1528.

29 H. Hayashi, W. Nihashi, T. Umeyama, Y. Matano, S. Seki, Y. Shimizu and H. Imahori, *J. Am. Chem. Soc.*, 2011, **133**, 10736–10739.

30 T. Lei, J. H. Dou, Z. J. Ma, C. H. Yao, C. J. Liu, J. Y. Wang and J. Pei, *J. Am. Chem. Soc.*, 2012, **134**, 20025–20028.

31 M. Schwoerer and H. C. Wolf, *Organic Molecular Solids*, WILEY-VCH Verlag GmbH & Co. KGaA, Weinheim, Germany, 2007.

32 S. V. Bhosale, C. H. Jani and S. J. Langford, *Chem. Soc. Rev.*, 2008, **37**, 331–342.

33 F. B. L. Cougnon, H. Y. Au-Yeung, G. D. Pantoş and J. K. M. Sanders, *J. Am. Chem. Soc.*, 2011, **133**, 3198–3207.

34 D. G. Hamilton, M. Montalti, L. Prodi, M. Fontani, P. Zanello and J. K. M. Sanders, *Chem. Eur. J.*, 2000, **6**, 608–617.

35 T. Iijima, S. A. Vignon, H. R. Tseng, T. Jarrosson, J. K. M. Sanders, F. Marchioni, M. Venturi, E. Apostoli, V. Balzani and J. F. Stoddart, *Chem. - A Eur. J.*, 2004, **10**, 6375–6392.

36 Y. Liu, L. M. Klivansky, S. I. Khan and X. Zhang, *Org. Lett.*, 2007, **9**, 2577–2580.

37 S. Nygaard, Y. Liu, P. C. Stein, A. H. Flood and J. O. Jeppesen, *Adv. Funct. Mater.*, 2007, **17**, 751–762.

38 M. Mamada, C. Parez-Bolivar and P. Jr. Anzenbacher, *Org. Lett.*, 2011, **13**, 4882–4885.

39 S. Nygaard, B. W. Laursen, T. S. Hansen, A. D. Bond, A. H. Flood and J. O.

Jeppesen, *Angew. Chemie - Int. Ed.*, 2007, **46**, 6093–6097.

40 Y. Liu, A. H. Flood, P. A. Bonvallet, S. A. Vignon, B. H. Northrop, H. R. Tseng, J. O. Jeppesen, T. J. Huang, B. Brough, M. Baller, S. Magonov, S. D. Solares, W. A. Goddard, C. M. Ho and J. Fraser Stoddart, *J. Am. Chem. Soc.*, 2005, **127**, 9745–9759.

41 K. A. Nielsen, W. S. Cho, J. Lyskawa, E. Levillain, V. M. Lynch, J. L. Sessler and J. O. Jeppesen, *J. Am. Chem. Soc.*, 2006, **128**, 2444–2451.

42 S. Nygaard, C. N. Hansen and J. O. Jeppesen, *J. Org. Chem.*, 2007, **72**, 1617–1626.

43 V. J. Bhanvadia and A. L. Patel, *New J. Chem.*, 2018, **42**, 17700–17707.

44 K. Kanakarajan and A. W. Czarnik, *J. Org. Chem.*, 1986, **51**, 5241–5243.

45 G. Nagarjuna, A. Kokil, J. Kumar and D. Venkataraman, *J. Mater. Chem.*, 2012, **22**, 16091–16094.

46 M. J. Frisch, G. W. Trucks, H. B. Schlegel, G. E. Scuseria, M. A. Robb, J. R. Cheeseman, G. Scalmani, V. Barone, B. Mennucci, G. A. Petersson, H. Nakatsuji, M. Caricato, X. Li, H. P. Hratchian, A. F. Izmaylov, J. Bloino, G. Zheng, J. L. Sonnenberg, M. Had and D. J. Fox, 2009.

47 S. J. Mahoney, M. M. Ahmida, H. Kayal, N. Fox, Y. Shimizu and S. H. Eichhorn, *J. Mater. Chem.*, 2009, **19**, 9221–9232.

48 T.-H. Chang, B.-R. Wu, M. Y. Chiang, S.-C. Liao, C. W. Ong, H.-F. Hsu and S. Lin, *Org. Lett.*, 2005, **7**, 4075–4078.

49 T. Van Der Boom, R. T. Hayes, Y. Zhao, P. J. Bushard, E. A. Weiss and M. R. Wasielewski, *J. Am. Chem. Soc.*, 2002, **124**, 9582–9590.

50 P. Xiao, F. Dumur, B. Graff, D. Gigmes, J. P. Fouassier and J. Lalevée, *Macromolecules*, 2013, **46**, 7661–7667.

51 M. Karikomi, C. Kitamura, S. Tanaka and Y. Yamashita, *J. Am. Chem. Soc.*, 1995, **117**, 6791–6792.

52 J. Chen, W. Wang, M. A. Reed, A. M. Rawlett, D. W. Price and J. M. Tour, *Appl. Phys. Lett.*, 2000, **77**, 1224–1226.

53 Y. Yamashita, K. Suzuki and M. Tomura, *Synth. Met.*, 2003, **133**–**134**, 341–343.

54 K. Pilgram, M. Zupan and R. Skiles, *J. Heterocycl. Chem.*, 2018, **7**, 629–633.

55 H. A. M. van Mullekom, J. A. J. M. Venkemans and E. W. Meijer, *Chem. Commun.*, 1996, 2163–2164.

56 J. Chen and Y. Cao, *Acc. Chem. Res.*, 2009, **42**, 1709–1718.

57 P.-L. T. Boudreault, A. Najari and M. Leclerc, *Chem. Mater.*, 2011, **23**, 456–469.

58 H. N. Tsao, D. M. Cho, I. Park, M. R. Hansen, A. Mavrinskiy, D. Y. Yoon, R. Graf, W. Pisula, H. W. Spiess and K. Müllen, *J. Am. Chem. Soc.*, 2011, **133**, 2605–2612.

59 C. B. Nielsen, B. C. Schroeder, A. Hadipour, B. P. Rand, S. E. Watkins and I. McCulloch, *J. Mater. Chem.*, 2011, **21**, 17642–17645.

60 T. Suzuki, H. Fujii, Y. Yamashita, C. Kabuto, S. Tanaka, M. Harasawa, T. Mukai and T. Miyashi, *J. Am. Chem. Soc.*, 1992, **114**, 3034–3043.

61 K. Ono, S. Tanaka and Y. Yamashita, *Angew. Chemie Int. Ed. English*, 1994, **33**, 1977–1979.

62 Y. Yamashita, M. Tomura and K. Imaeda, *Chem. Commun.*, 1996, 2021–2022.

63 Y. Yamashita, K. Ono, M. Tomura and K. Imaeda, *Chem. Commun.*, 1997, 1851–1852.

64 J.-M. Raimundo, P. Blanchard, H. Brisset, S. Akoudad and J. Roncali, *Chem. Commun.*, 2000, 939–940.

65 M. T. S. Ritonga, H. Sakurai and T. Hirao, *Tetrahedron Lett.*, 2002, **43**, 9009–9013.

66 J. Huang, Y. Niu, W. Yang, Y. Mo, M. Yuan and Y. Cao, *Macromolecules*, 2002, **35**, 6080–6082.

67 P. F. Xia, J. Lu, C. H. Kwok, H. Fukutani, M. S. Wong and Y. Tao, *J. Polym. Sci. Part A Polym. Chem.*, 2008, **47**, 137–148.

68 Y. Yang, Y. Zhou, Q. He, C. He, C. Yang, F. Bai and Y. Li, *J. Phys. Chem. B*, 2009, **113**, 7745–7752.

69 G. D. Sharma, P. Suresh, M. S. Roy and J. A. Mikroyannidis, *J. Power Sources*, 2010, **195**, 3011–3016.

70 S. Beaupré and M. Leclerc, *J. Mater. Chem. A*, 2013, **1**, 11097–11105.

71 J. Peet, J. Y. Kim, N. E. Coates, W. L. Ma, D. Moses, A. J. Heeger and G. C. Bazan, *Nat. Mater.*, 2007, **6**, 497.

72 P. Zhou, Z.-G. Zhang, Y. Li, X. Chen and J. Qin, *Chem. Mater.*, 2014, **26**, 3495–3501.

73 L. Fan, R. Cui, X. Guo, D. Qian, B. Qiu, J. Yuan, Y. Li, W. Huang, J. Yang, W. Liu, X. Xu, L. Li and Y. Zou, *J. Mater. Chem. C*, 2014, **2**, 5651–5659.

74 C. B. Nielsen, R. S. Ashraf, N. D. Treat, B. C. Schroeder, J. E. Donaghey, A. J. P. White, N. Stingelin and I. McCulloch, *Adv. Mater.*, 2014, **27**, 948–953.

75 L. Ye, S. Zhang, W. Zhao, H. Yao and J. Hou, *Chem. Mater.*, 2014, **26**, 3603–3605.

76 H. Zhou, L. Yang, A. C. Stuart, S. C. Price, S. Liu and W. You, *Angew. Chemie Int. Ed.*, 2011, **50**, 2995–2998.

77 B. C. Schroeder, R. S. Ashraf, S. Thomas, A. J. P. White, L. Biniek, C. B. Nielsen, W. Zhang, Z. Huang, P. S. Tuladhar, S. E. Watkins, T. D. Anthopoulos, J. R. Durrant and I. McCulloch, *Chem. Commun.*, 2012, **48**, 7699–7701.

78 H. Bronstein, J. M. Frost, A. Hadipour, Y. Kim, C. B. Nielsen, R. S. Ashraf, B. P. Rand, S. Watkins and I. McCulloch, *Chem. Mater.*, 2013, **25**, 277–285.

79 J. A. Love, I. Nagao, Y. Huang, M. Kuik, V. Gupta, C. J. Takacs, J. E. Coughlin, L. Qi, T. S. van der Poll, E. J. Kramer, A. J. Heeger, T.-Q. Nguyen and G. C. Bazan, *J. Am. Chem. Soc.*, 2014, **136**, 3597–3606.

80 T. Qin, W. Zajaczkowski, W. Pisula, M. Baumgarten, M. Chen, M. Gao, G. Wilson, C. D. Easton, K. Müllen and S. E. Watkins, *J. Am. Chem. Soc.*, 2014, **136**, 6049–6055.

81 L. Wang, D. Cai, Q. Zheng, C. Tang, S.-C. Chen and Z. Yin, *ACS Macro Lett.*, 2013, **2**, 605–608.

82 H. Li, T. M. Koh, A. Hagfeldt, M. Grätzel, S. G. Mhaisalkar and A. C. Grimsdale, *Chem. Commun.*, 2013, **49**, 2409–2411.

83 J. a. Mikroyannidis, M. M. Stylianakis, P. Suresh, P. Balraju and G. D. Sharma, *Org. Electron. physics, Mater. Appl.*, 2009, **10**, 1320–1333.

84 J. a. Mikroyannidis, P. Suresh and G. D. Sharma, *Org. Electron. physics, Mater. Appl.*, 2010, **11**, 311–321.

85 J. a. Mikroyannidis, M. M. Stylianakis, Q. Dong, Y. Zhou and W. Tian, *Synth. Met.*, 2009, **159**, 1471–1477.

86 T. Xu and Q. Qiao, *Energy Environ. Sci.*, 2011, **4**, 2700–2720.

87 J. Bouclé, P. Ravirajan and J. Nelson, *J. Mater. Chem.*, 2007, **17**, 3141–3153.

88 B. de Boer, A. Hadipour, M. M. Mandoc, T. van Woudenbergh and P. W. M. Blom, *Adv. Mater.*, 2005, **17**, 621–625.

89 G. Heimel, L. Romaner, E. Zojer and J.-L. Brédas, *Nano Lett.*, 2007, **7**, 932–940.

90 J. Yu, T.-L. Shen, W.-H. Weng, Y.-C. Huang, C.-I. Huang, W.-F. Su, S.-P. Rwei, K.-C. Ho and L. Wang, *Adv. Energy Mater.*, 2011, **2**, 245–252.

91 S.-J. Moon, E. Baranoff, S. M. Zakeeruddin, C.-Y. Yeh, E. W.-G. Diau, M. Grätzel and K. Sivula, *Chem. Commun.*, 2011, **47**, 8244–8246.

92 G. K. Mor, S. Kim, M. Paulose, O. K. Varghese, K. Shankar, J. Basham and C. A. Grimes, *Nano Lett.*, 2009, **9**, 4250–4257.

93 W. Zhang, R. Zhu, F. Li, Q. Wang and B. Liu, *J. Phys. Chem. C*, 2011, **115**, 7038–7043.

94 R. Zhu, C. Y. Jiang, B. Liu and S. Ramakrishna, *Adv. Mater.*, 2009, **21**, 994–1000.

95 V. J. Bhanvadia, H. A. Patel, N. N. Sharma and A. L. Patel, *Synth. Commun.*,

2016, **46**, 1052–1061.

96 B. A. D. Neto, A. S. Lopes, G. Ebeling, R. S. Goncalves, V. E. U. Costa, F. H. Quina and J. Dupont, *Tetrahedron*, 2005, **61**, 10975–10982.